Applications of microwave radiometry in ocean and atmospheric science

Peter J Minnett
Rosenstiel School of Marine and Atmospheric Science,
University of Miami, USA

UNIVERSITY OF MIAMI
ROSENSTIEL SCHOOL of MARINE & ATMOSPHERIC SCIENCE

ESA EARTH OBSERVATION SUMMER SCHOOL
ON EARTH SYSTEM MONITORING & MODELLING
30 July - 10 August 2012

esa

Outline

- Review Planck function –Rayleigh Jeans Approximation
- What are oceanographic and atmospheric signals detectable from space?
- Instrument descriptions
  - SSM/I
  - TMI
  - AMSR-E
- Examples of measurements
- New salinity mission - Aquarius

Rayleigh-Jeans

Rayleigh-Jeans Law corresponds to the Planck Law in the case of low frequencies, in which case (hν)/(kT)<< 1 allows the approximation

$$e^{h\nu/(kT)} \approx 1 + \frac{h\nu}{kT} + \ldots.$$

Putting this into the Planck law gives

$$R_\nu(T) \approx \frac{2\nu^3 h}{c^2} \frac{1}{(1 + \frac{h\nu}{kT} + \ldots) - 1}$$

$$= \frac{2\nu^2 kT}{c^2}.$$

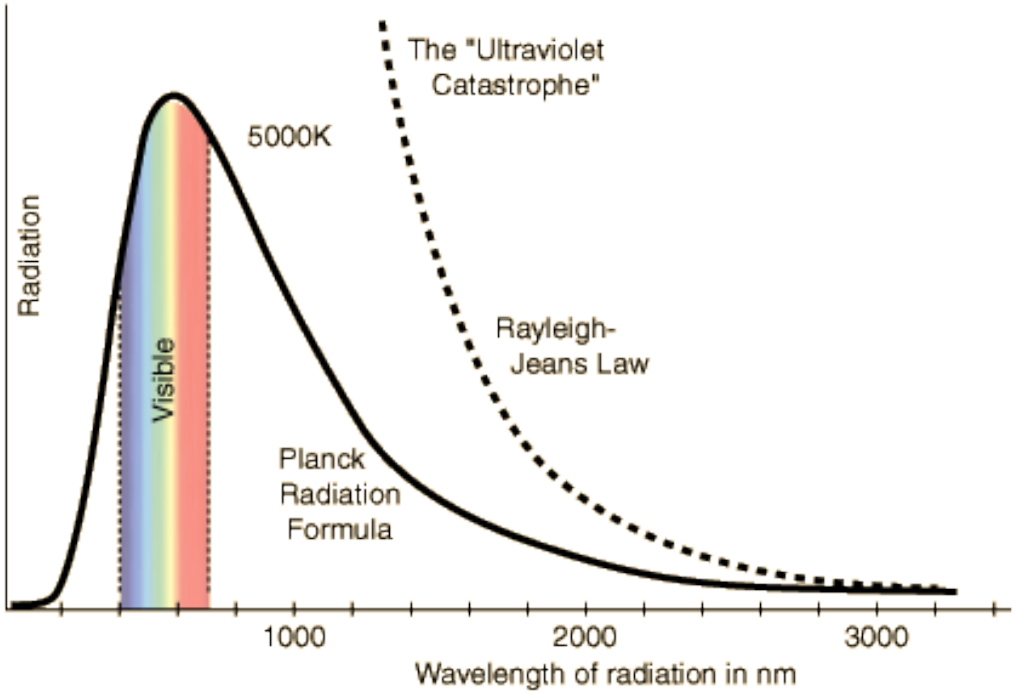

See http://hyperphysics.phy-astr.gsu.edu/hbase/mod6.html

Microwave part of the spectrum

The microwave region of the electromagnetic spectrum ranges from about 300 MHz to 300 GHz (wavelengths from 1 meter to 1 mm).

Scattering regimes

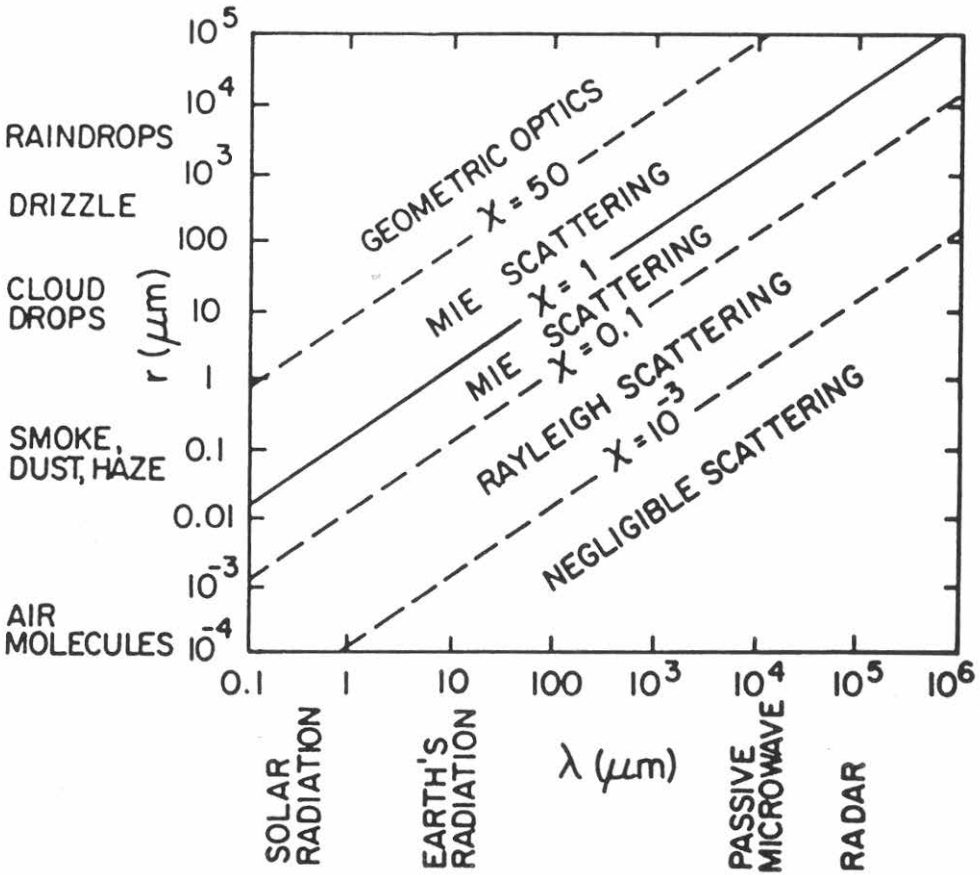

Scattering regimes. [Adapted from Wallace and Hobbs (1977).

$\chi = 2\pi a / \lambda$

$= q$

Microwave brightness temperature dependences

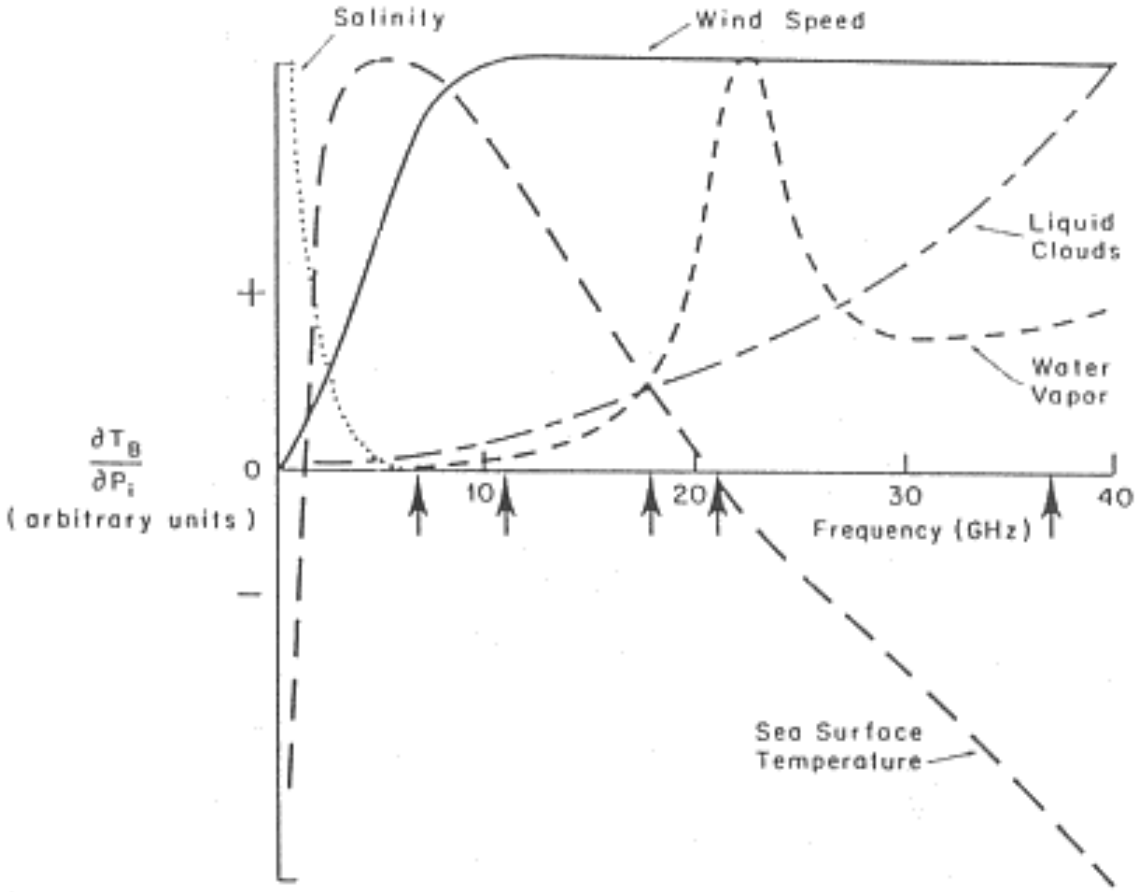

Sketch of the variations of brightness temperatures (T_B) measured by satellite–borne microwave radiometers as a function of various geophysical parameters. The arrows show the frequencies of the channels of the Scanning Multichannel Microwave Radiometer (SMMR). After Wilheit et al., 1980.

Microwave sensitivities

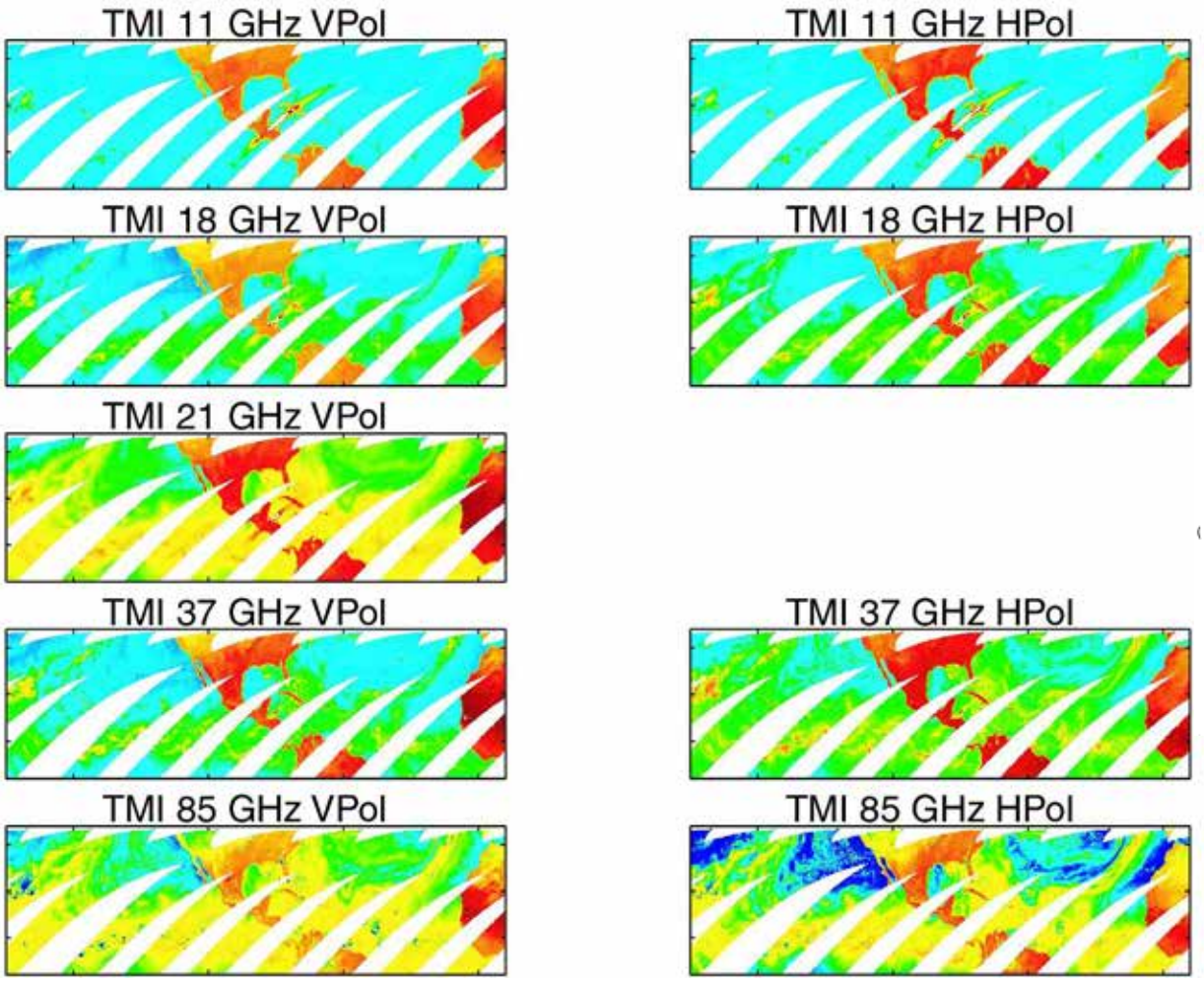

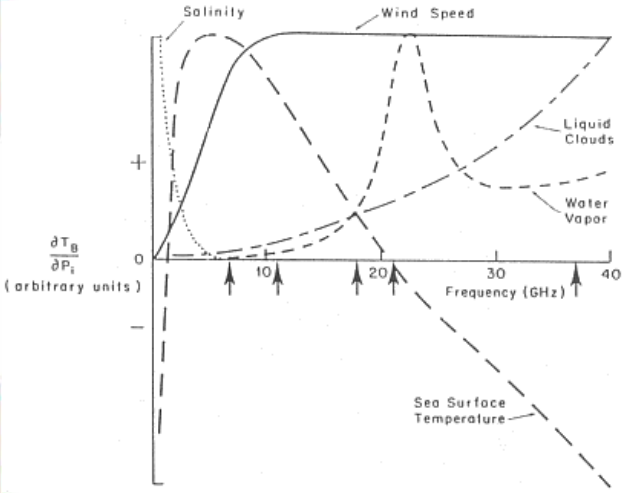

From Chelle Gentemann, Remote Sensing Systems.

Microwave radiometers

Electrically Scanning Microwave Radiometer (ESMR) on Nimbus 5 (1973-1976)

Scanning Multichannel Microwave Radiometer (SMMR) on SeaSat (1978) & Nimbus 7 (1978-1987).

Special Sensor Microwave Imager (SSM/I) on DMSP Series (1987 ….)

TRMM (Tropical Rainfall Measuring Mission) Microwave Imager (TMI) on TRMM (1998…)

Advanced Microwave Scanning Radiometer (AMSR-E) on Aqua (2002-2011)

Advanced Microwave Scanning Radiometer (AMSR) on Midori (2002-2003)

Special Sensor Microwave Imager/Sounder (SSMIS) on DMSP F-16 (2005….)

Advanced Technology Microwave Scanner (ATMS) on NPP (2011…)

Advanced Microwave Scanning Radiometer-2 (AMSR-2) on GCOM-W (2012…)

Microwave antenna patterns

The spatial resolution is diffraction limited by the antenna size and the wavelength.

This gives rise to side-lobe contamination. The strong contrast near boundaries, such as coasts, means significant errors can occur.

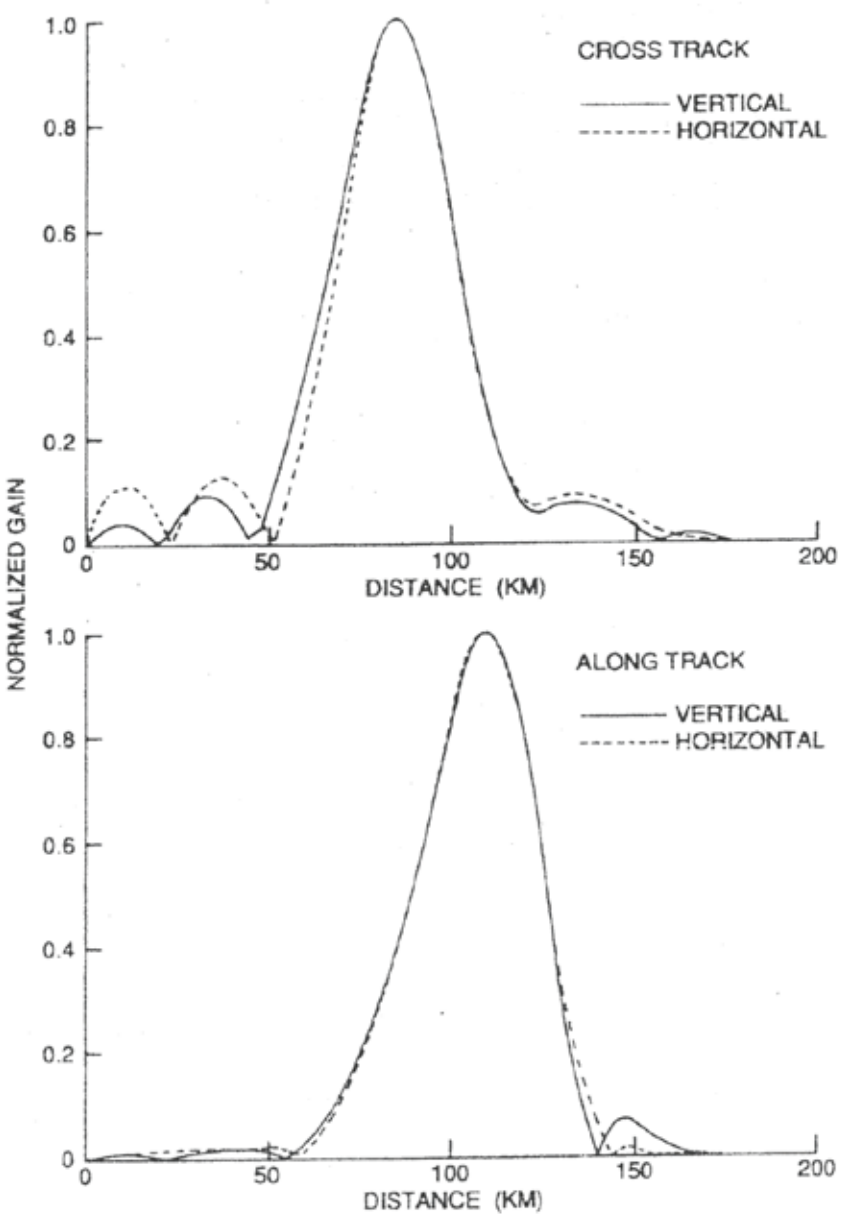

37 GHz antenna gain function derived from coastline overpasses.

SSM/I

- Measures microwave energy emitted from the surface of the earth or atmosphere.
- Conical scan which results in a constant zenith angle of 53.1^{o} at the surface of the earth.
- The swath width is about 1400 km, about half of width of the corresponding visible and infrared swaths.
- Measures at four frequencies, three of which are dual-polarized: vertical & horizontal. The brightness temperature differences between the horizontal and vertical polarizations often give useful information about meteorological and surface phenomena.

SSM/I Channels

Abbreviation	Frequency (GHz)	Resolution (km)
19V	19.35	70x45
19H	19.35	70x45
22V	22.235	60x40
37V	37.0	38x30
37H	37.0	38x30
85V	85.5	16x14
85H	85.5	16x14

V = Vertical polarization

H = Horizontal polarization

SSM/I scan

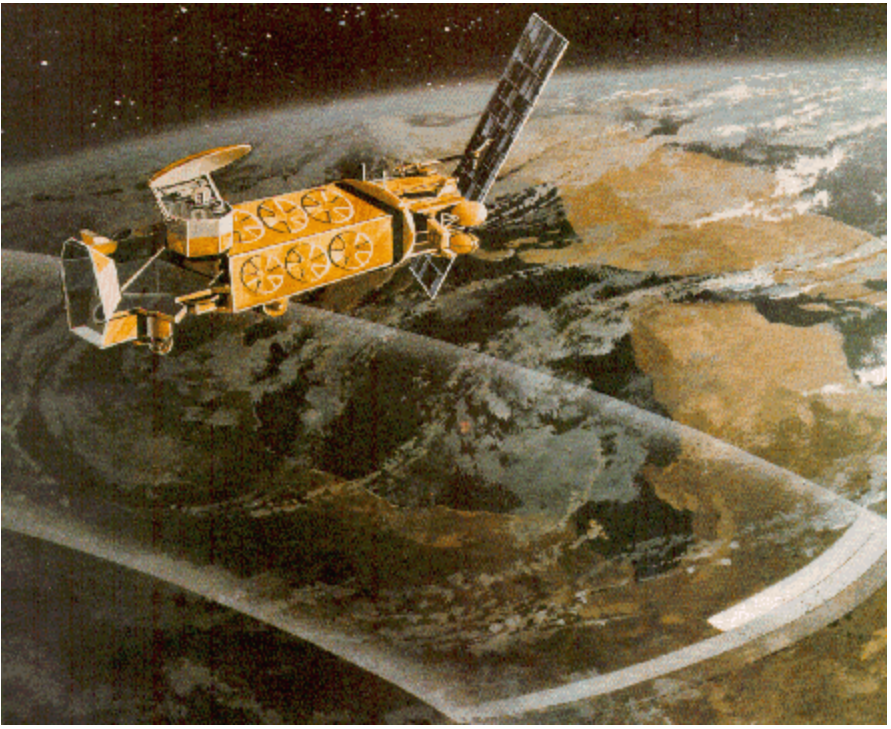

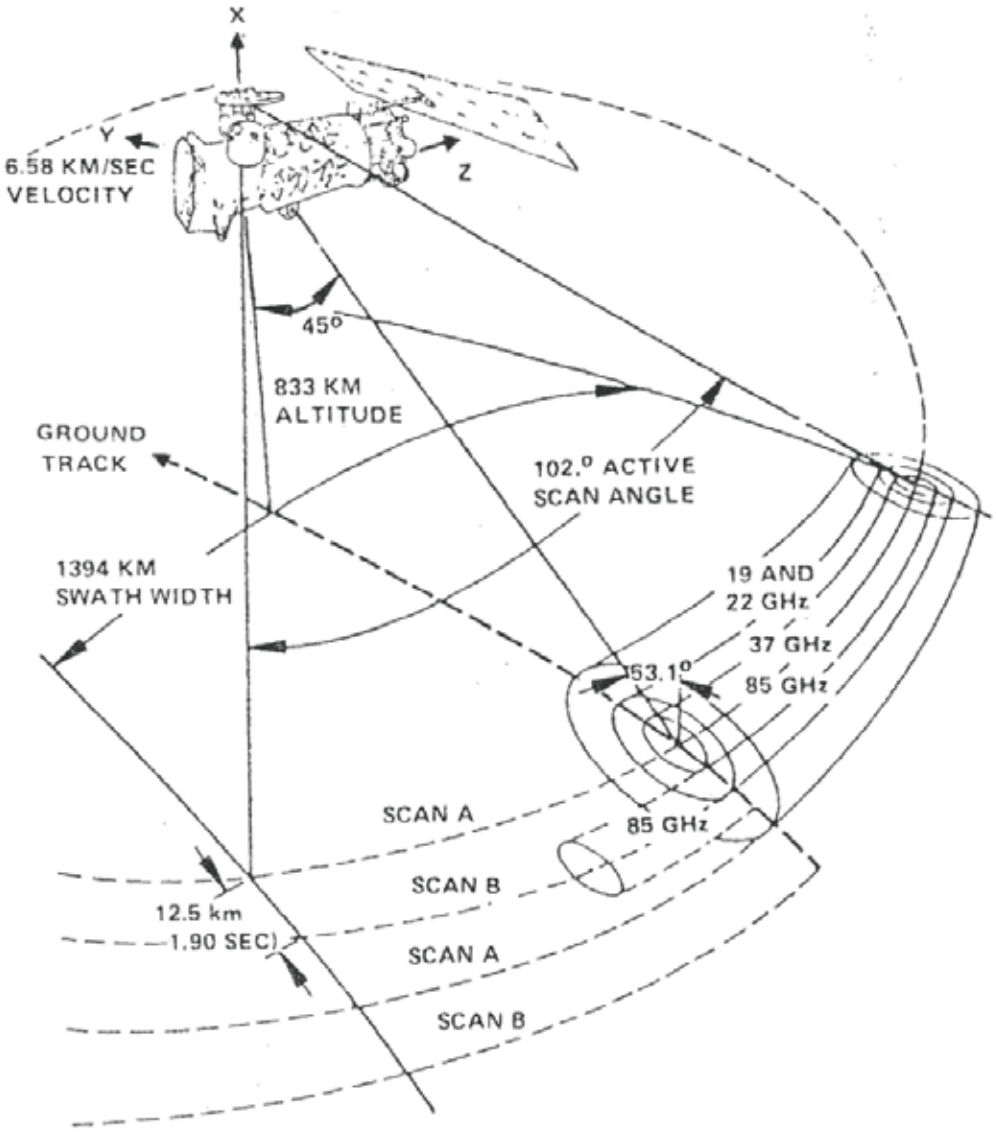

Fig. 4. SSM/I scan geometry.

DMSP orbit

SSM/I coverage
in a 24h period

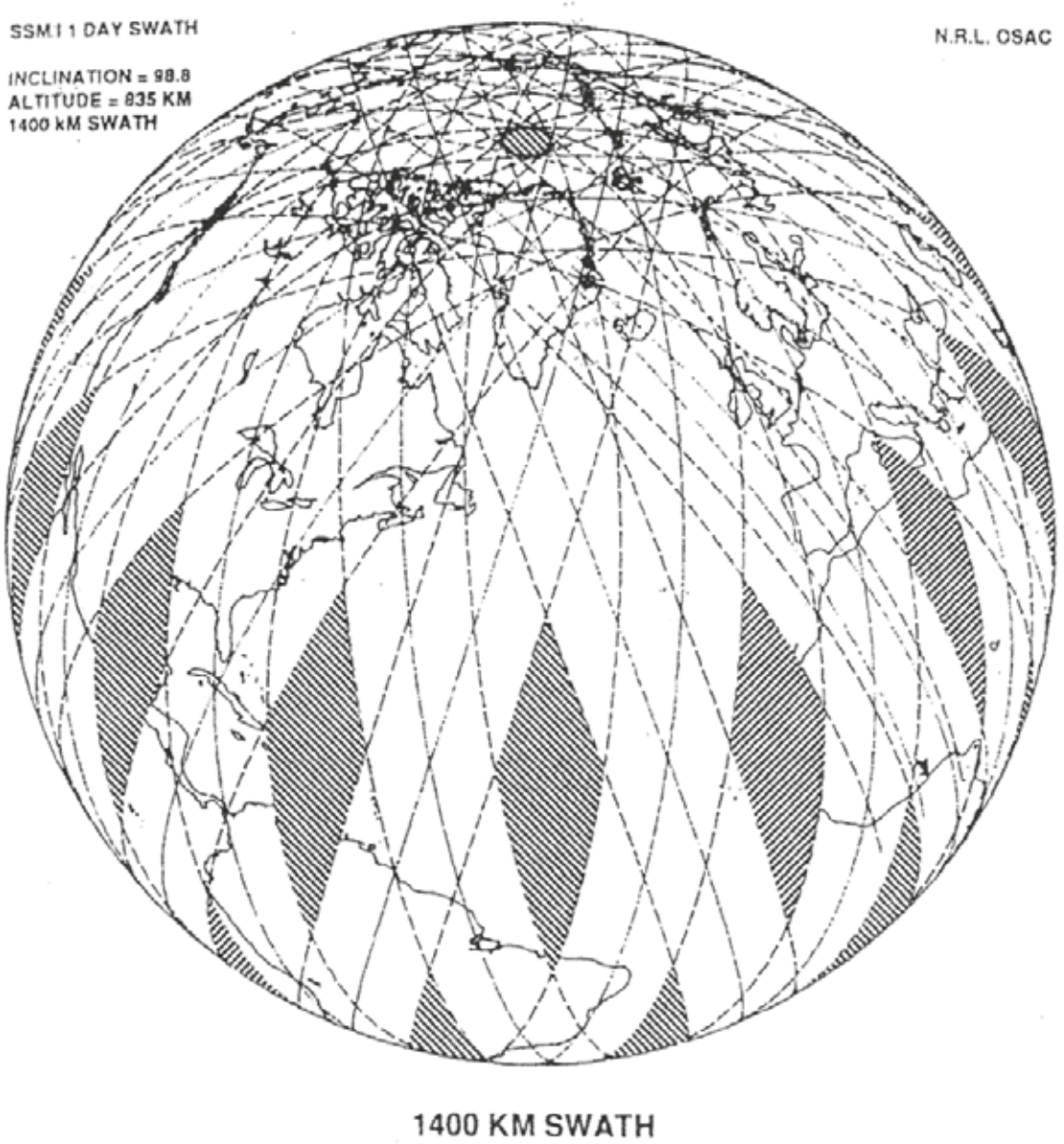

Fig. 2. Earth coverage of the SSM/I in a 24 h period. Only the shaded areas are not observed in this time period.

SSM/I ocean surface winds.

The wind speed algorithm developed by Goodberlet et al. (1989):

$$WS = 147.90 + 1.0969 * TB_{19v} - 0.4555 * TB_{22v} - 1.7600 * TB_{37v} + 0.7860 * TB_{37h}$$

where TB is the radiometric brightness temperature at the frequencies and polarizations indicated.

All data where $TB_{37v} - TB_{37h} < 50K$ or $TB_{19h} > 165K$ are flagged.

Goodberlet, M. A., Swift, C. T. and Wilkerson, J. C., "Remote Sensing of Ocean Surface Winds With the Special Sensor Microwave/Imager", J. Geophys. Res.,94, 14574-14555, 1989

Wind Speed

The microwave wind speed retrieval estimates the ocean wind speed by sensing the roughness of the ocean's surface caused by the surface wind. It does not give wind direction. Unless there is precipitation, the accuracy of the wind speed is 2 ms^{-1} or better.

Wind speeds are not reliable >~20 ms^{-1} (40 kt). Thus, the microwave wind speeds can not be used for intense storm systems or tropical cyclones. In these storms, rain contamination and high winds often combine to render the microwave radiometer winds nearly useless.

Near coastlines, microwave side-lobe contamination makes the speeds useless. Values are only valid further away than about 50 nm (80 km) from shore. Sometimes on wind speed images this effect will be seen as a "fringe" or "ring" of higher values surrounding coastlines and islands. These are invalid wind speed estimates.

Wind Speed

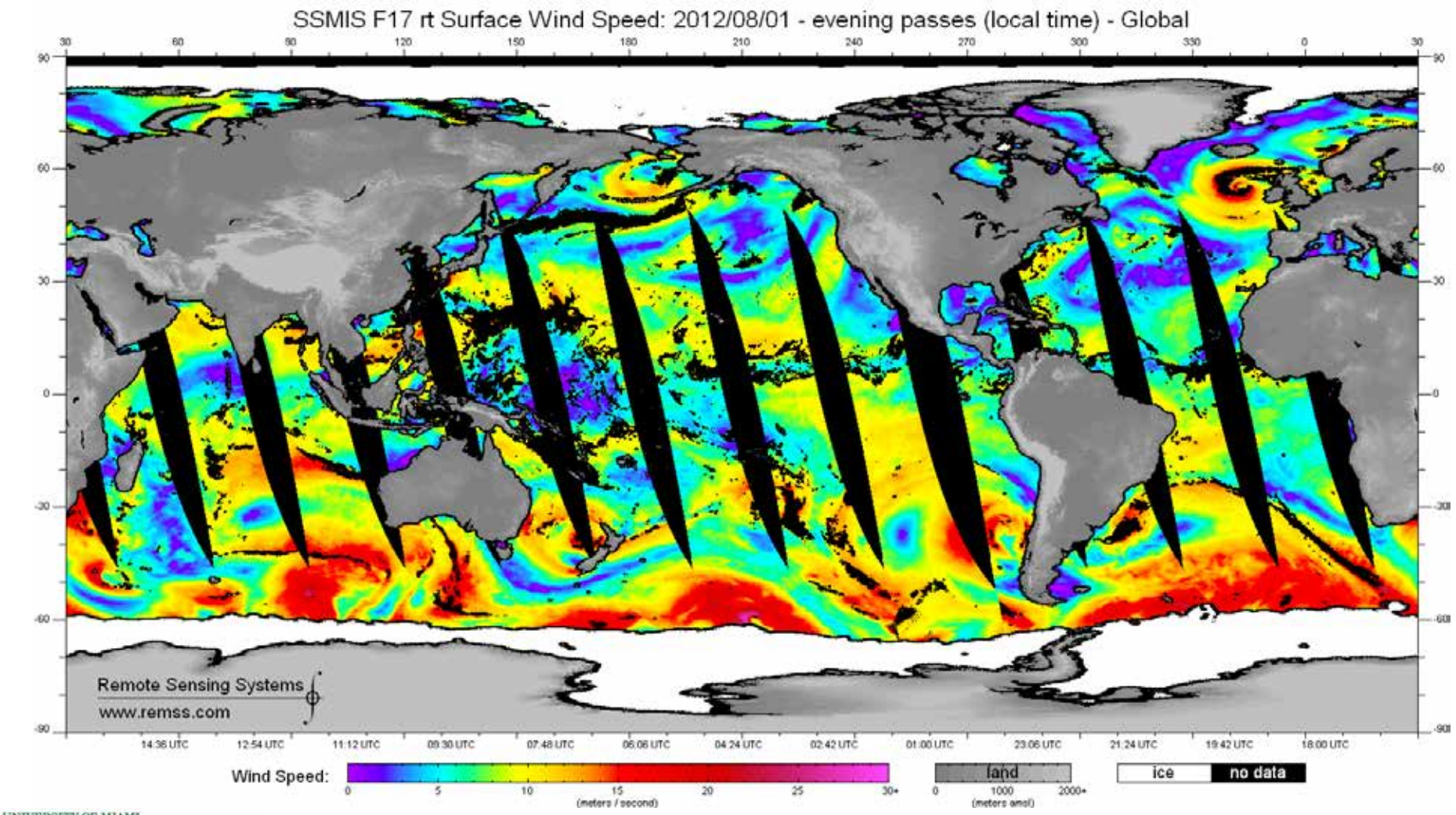
SSMIS F17 rt Surface Wind Speed: 2012/08/01 - evening passes (local time) - Global
Remote Sensing Systems
www.remss.com
Wind Speed:
(meters / second)
land
(meters amsl)
ice
no data

Integrated water vapor

Gives the total amount of water vapor in a column above a unit area from the surface of the ocean to the top of the atmosphere. Since the marine boundary layer (roughly the lowest 1 km of the atmosphere) usually holds the bulk of the water vapor, the integrated water vapor parameter heavily represents vapor in the boundary layer.

It is generally considered to be as accurate as radiosonde values of integrated vapor.

This parameter is useful over water only. Side-lobe contamination within about 50 nm (80 km) to coastlines or islands.

$$WV = a_0 + a_1 T_{19V} + a_2 T_{22V} + a_3 T_{37V} + a_4 (T_{22V})^2$$

$a_0 = 232.89292$ $a_1 = -0.148596$ $a_2 = -1.829125$ $a_3 = -0.36954$
$a_4 = 0.006193$ (sign wrong in referenced paper)

Alishouse, J. C., S. A. Snyder, J. Vongsathorn, and R. R. Ferraro, 1990: Determination of oceanic total precipitable water from SSM/I. IEEE Trans. Geoscience and Remote Sensing, 28, 811-816.

Integrated water vapor

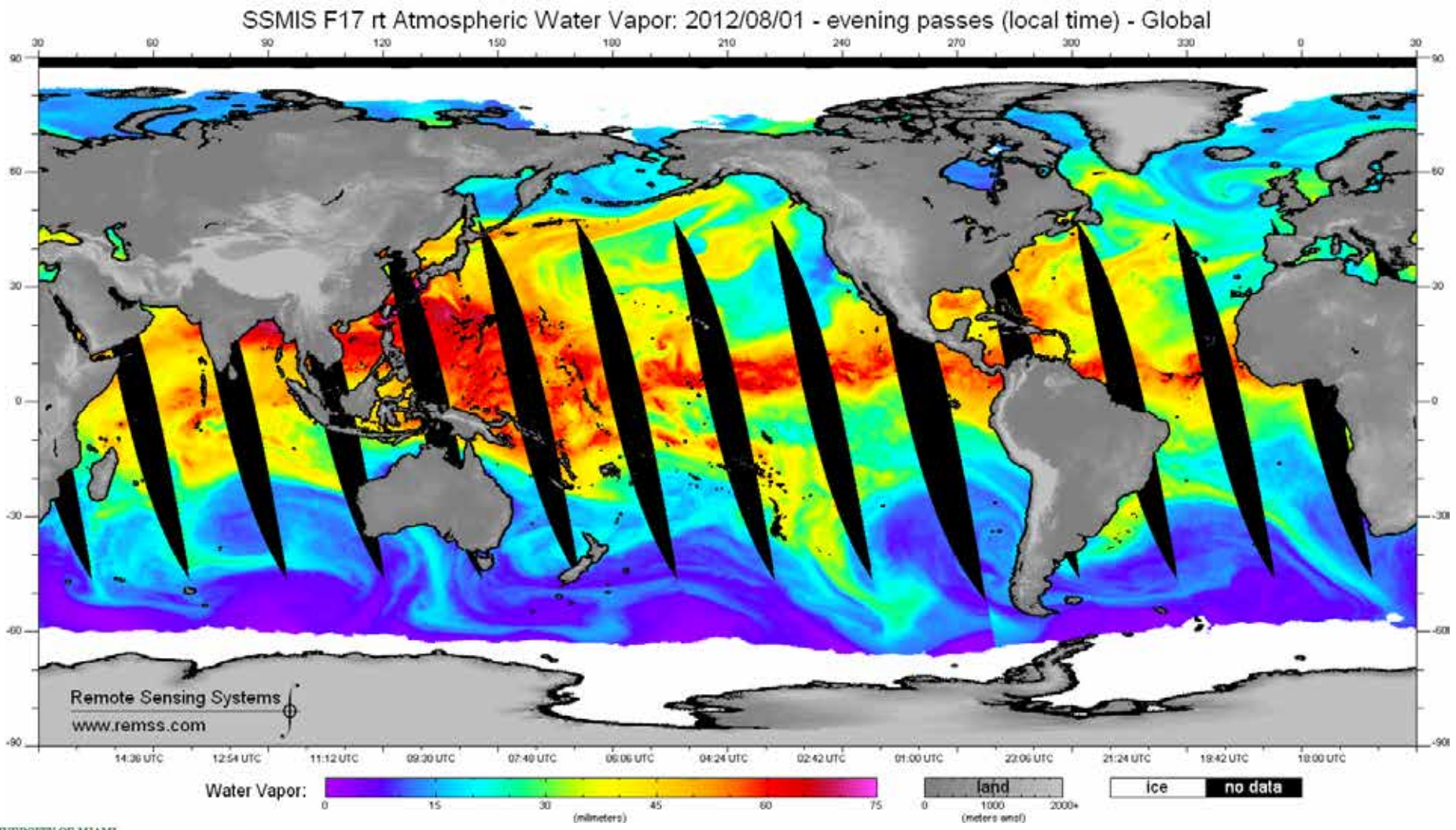

Water vapor from AMSR-E

Loop from Remote Sensing Systems http://www.remss.com/

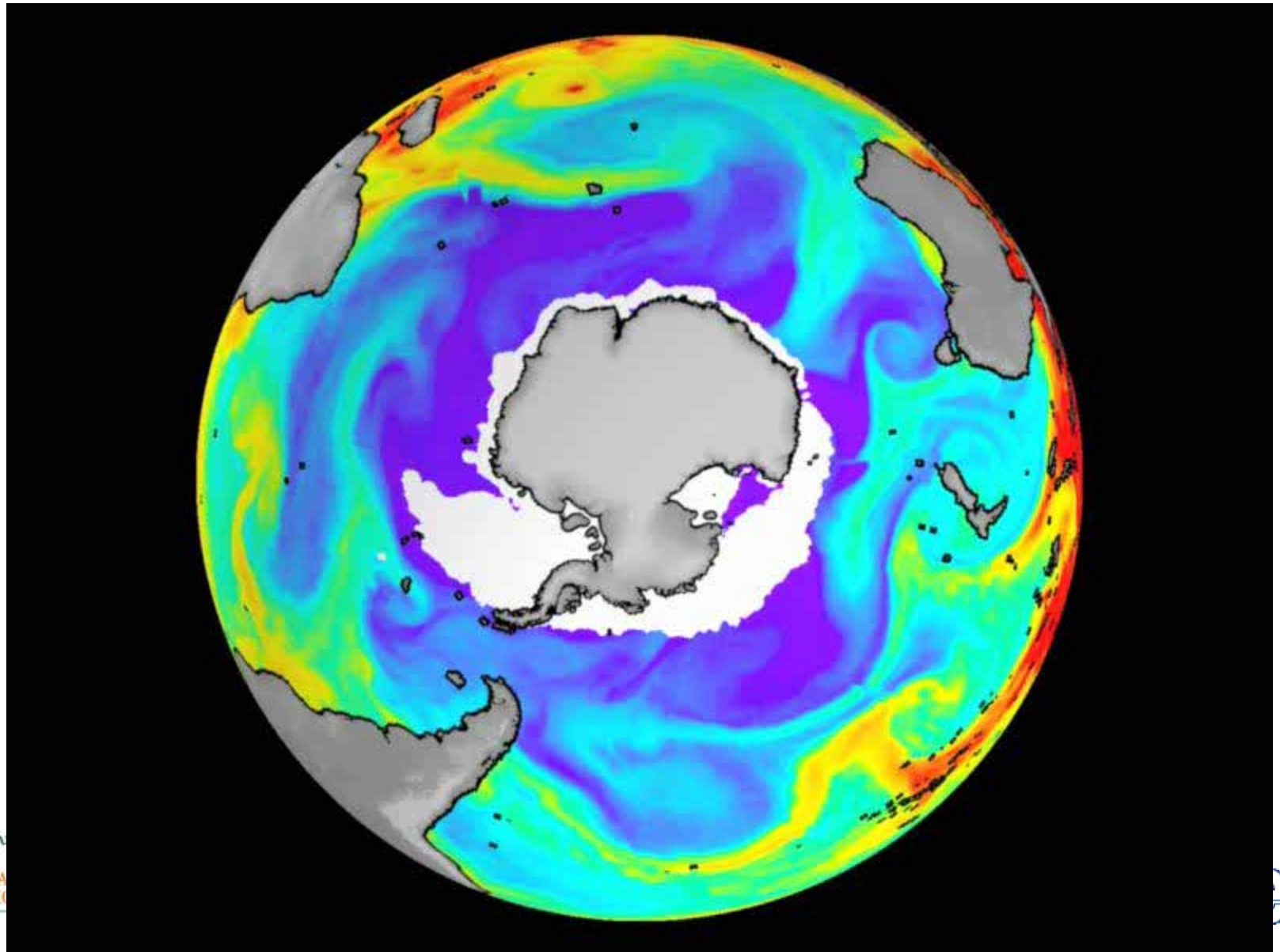

Integrated Liquid Water

Depth of liquid water from the surface of the ocean to the top of the atmosphere. Integrated liquid water has magnitudes one or two orders of magnitude less than integrated water vapor. It is measured in kg m^{-2}.

It is also sometimes called cloud water because liquid water is responsible for low-level clouds, e.g. stratus, stratocumulus, cumulus, and fog. Therefore, integrated liquid water measures the water content of clouds that are responsible for much of the weather experienced in the lowest few kilometers of the marine atmosphere.

Images yield patterns that should match water cloud patterns produced on more conventional satellite images, such as daytime visible images.

The integrated liquid water parameter has several disadvantages. First, it is not as accurate as some of the other marine parameters, notably integrated water vapor and surface wind speed. Most validation studies of this parameter have been performed over uniform marine stratus with relatively low liquid water contents. Thus, it is relatively untested in cloud systems with large liquid water contents. Large values of this parameter indicate precipitation and mark regions where the retrieved values are not accurate.

The liquid water parameter may have difficulty with thin water clouds of low water content and may not be able to distinguish these cloud systems from a cloud-free ocean background.

$$CLW = \Sigma a_i T_i \quad i=1,7$$

Alishouse *et al*, 1990. Determination of cloud liquid water using SSM/I. IEEE Trans. Geoscience and Remote Sensing, 28, 817-822.

Integrated Liquid Water

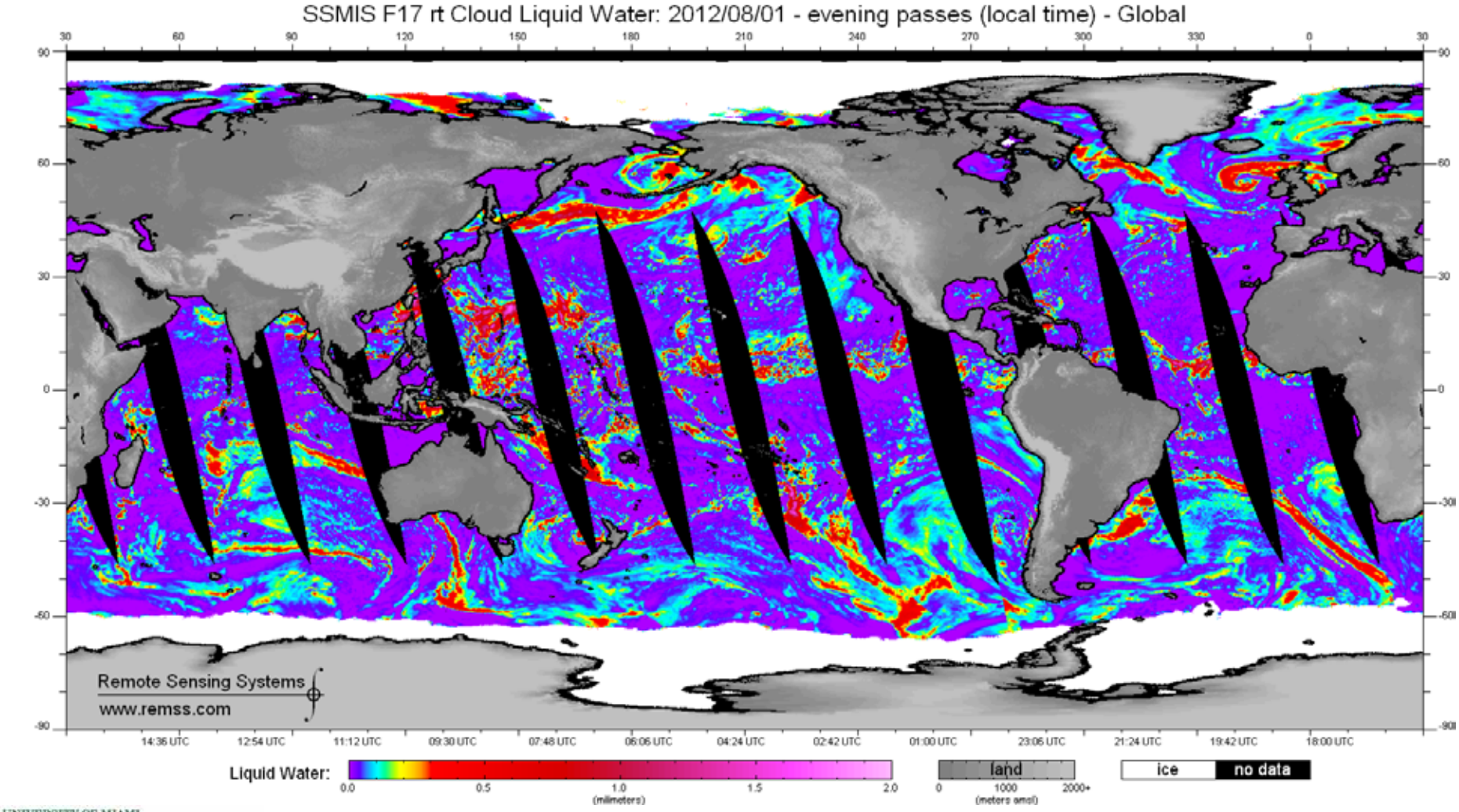

Convective (Cold) Rain

There are two basic mechanisms responsible for the ability to image precipitation at the SSM/I frequencies. Scattering by precipitation-sized ice particles above the freezing level causes microwave radiometers to register lower brightness temperatures than the cloud background. Emission by raindrops below the freezing level produces warmer brightness temperatures than in the surrounding areas. The ability to image convective precipitation depends of the scattering signature. The scattering flag is based on the 85 GHz channels, which have high spatial resolution. Thus, relatively small-scale detail such as convective cores within thunderstorms can be identified.

There are two main disadvantages to the microwave convective scattering flag. First, it cannot be used to estimate the quantitative amount of precipitation that is falling. In fact, it may not even tell whether precipitation is reaching the ground at all. Convective precipitation may be falling aloft and produce a signature on a convective scattering flag image, but may evaporate before reaching the ground. Another difficulty is that some precipitation systems may not have an important ice phase aloft but still be producing rain at a significant rate near the surface. The convective scattering flag may not identify these systems well. Over open oceans the convective rain flag may be supplemented with the stratiform flag. Thus, if rain without a overlying ice phase is occurring, the stratiform flag can provide the information the convective scattering flag missed. However, over land there is no way of ascertaining how much stratiform rain might be missed by the convective precipitation flag, since the stratiform flag does not operate there.

Stratiform (Warm) Rain

The stratiform rain flag is based on the 37 GHz (horizontal polarization) channel with brightness temperatures greater than 190 K. It can distinguish clouds without rain (or which contain only drizzle) from those which contain significant precipitation. It is valid over water only. The stratiform rain flag only tells whether rain is probably occurring in a given region; it does not indicate the rain rate. There are algorithms developed in the research community that do give rain rate; however, these are of limited accuracy.

The stratiform rain flag is based on the signal given off by rain drops near the surface of the ocean. Therefore unlike the convective rain flag which senses snowflakes above the freezing level, the stratiform rain flag senses information in the lowest portions of precipitating cloud systems. Accordingly, if there is precipitation aloft in a cloud system in the form of snowflakes, but this precipitation evaporates before melting, the stratiform rain flag will not detect the precipitation.

The stratiform rain flag has several disadvantages:

- it is only useful over ocean.
- it can only flag probable precipitation; it can not give rain rate.
- it may not distinguish well between drizzle and heavier rain.
- it is based on the 37 GHz channel which has a large footprint size. Thus, precipitation over a small portion of the pixel may not register as rain.

Rain rate

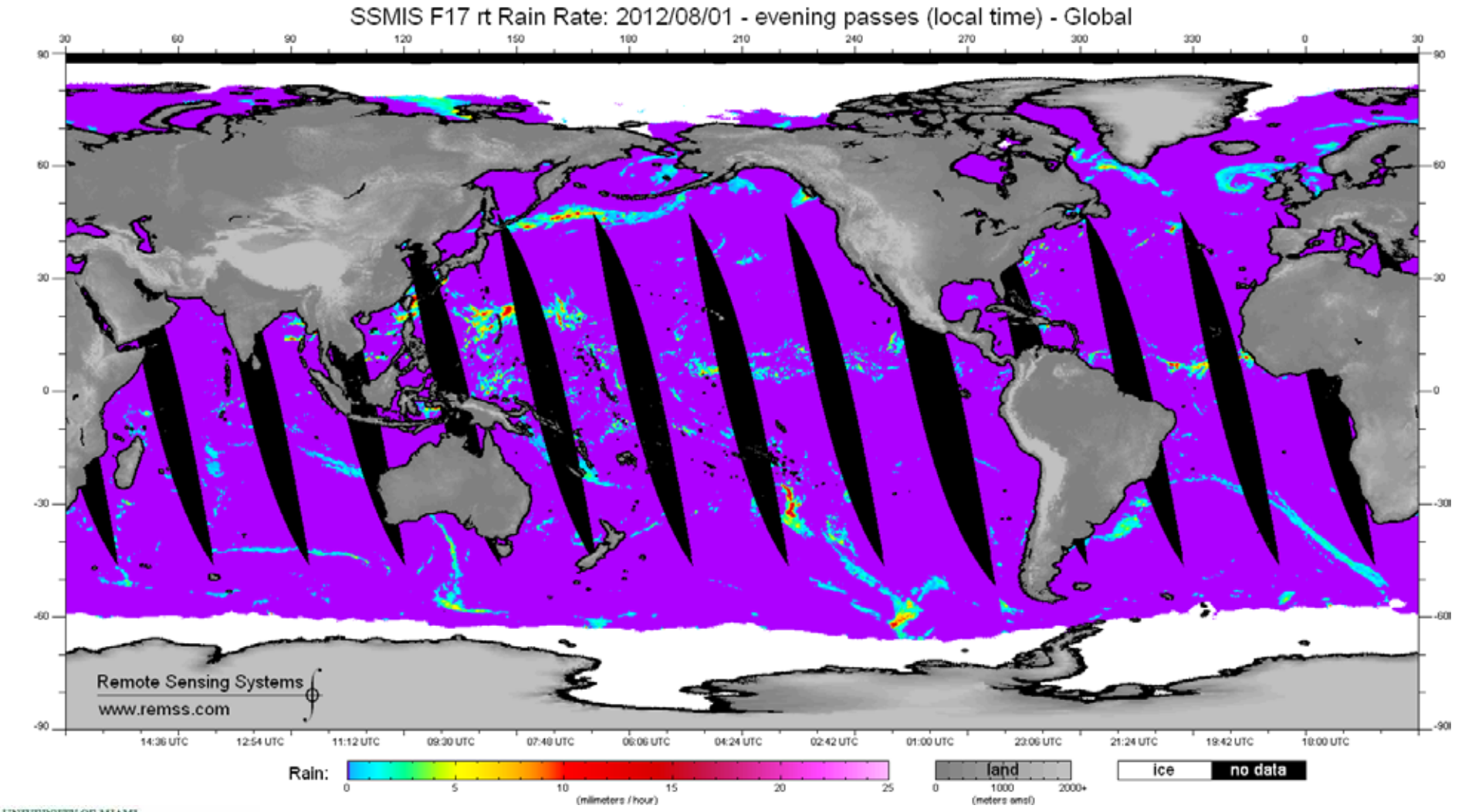
SSMIS F17 rt Rain Rate: 2012/08/01 - evening passes (local time) - Global
Remote Sensing Systems
www.remss.com
14:36 UTC
12:54 UTC
11:12 UTC
09:30 UTC
07:48 UTC
06:06 UTC
04:24 UTC
02:42 UTC
01:00 UTC
23:06 UTC
21:24 UTC
19:42 UTC
18:00 UTC
Rain:
0
5
10
15
20
25
(millimeters / hour)
land
0
1000
2000+
(meters amsl)
ice
no data

Retrieval errors

- Retrieval of geophysical parameters is a combination of the measured brightness temperatures, so errors in the retrievals can be correlated.
- Rather than independent retrievals, all can be retrieved in one algorithm: Wentz, F. J., 1997. A well-calibrated ocean algorithm for SSM/I, *Journal of Geophysical Research*, 102, 8703-8718.

Sea Ice

Microwave radiometry gives useful information about sea ice coverage at a resolution of 25 km to 6km.

Exploits the emissivity differences between sea ice and open water.

Unlike visible and infrared satellite images, it can be used in all seasons and at all times of day, independent of clouds. It can show the ice edge with a high degree of accuracy.

Since ice coverage changes fairly slowly (in comparison with meteorological changes), the twice-a-day coverage can give a relatively complete depiction of ice edge position at a given location.

There are several disadvantages of the microwave sea ice cover:

- water clouds, prevalent in some polar areas during the summer, can degrade the quality of sea ice retrievals.
- cannot resolve small ice floes or ice bergs of interest to navigation.
- while the ice edge is usually specified very accurately, the total ice coverage at a specific point is often not accurate because the differing emissivities of sea ice are sometimes not accounted for well in algorithms

Infrared and Microwave Brightness Temperatures

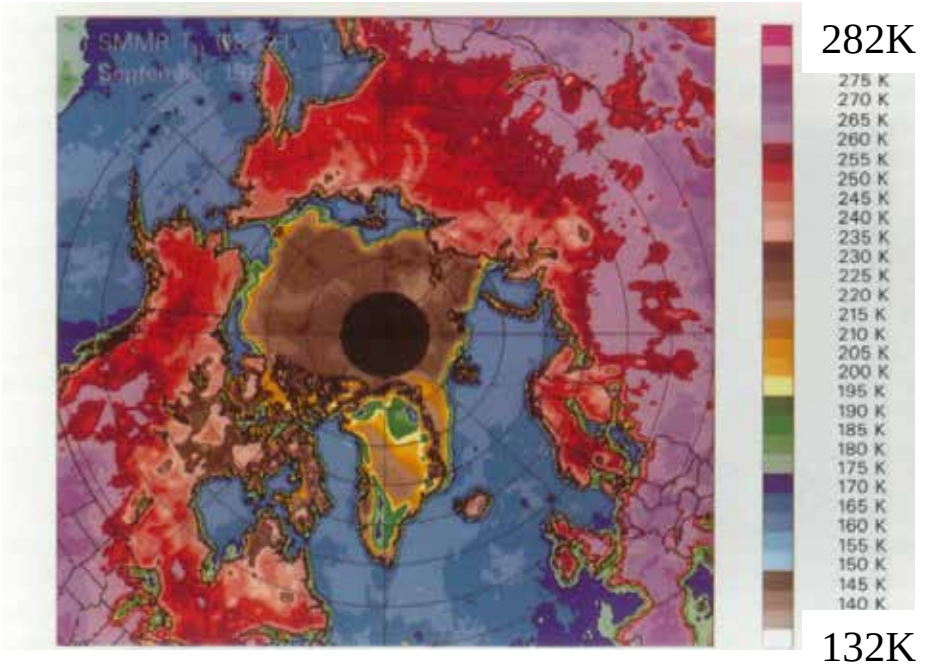

SMMR 18 GHz

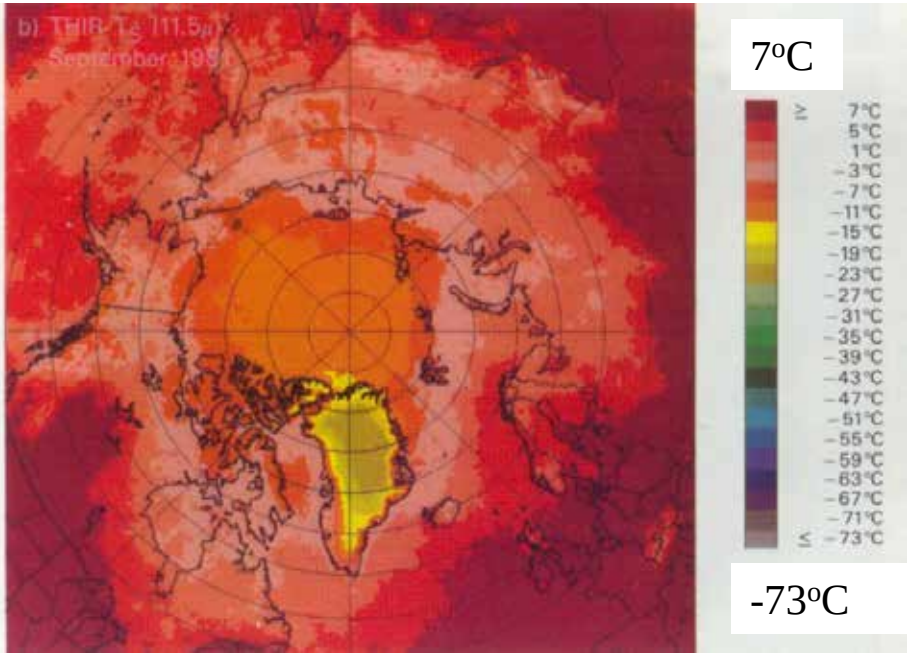

AVHRR 11.5 μm

September 1981

Much more contrast in microwave than thermal infrared - more information available in the microwave measurements.

Microwave emissivity of ice

Ice type	Pol.	4.9	6.7	10	18.7	21	37	90	94
Water	V	0.505 (0.015)	0.513 (0.015)	0.532 (0.015)	0.570 (0.033)	0.617 (0.015)	0.662 (0.029)	0.792 (0.019)	0.753 [0.026]
	H	0.253 (0.015)		0.295 (0.020)	0.332 (0.018)	0.332 (0.018)	0.392 (0.015)	0.528 (0.022)	0.488 [0.050]
New	V	0.560		0.568	0.623		0.703	0.850	
	H	0.280		0.315	0.368		0.417	0.573	
Nilas (dark)	V			0.705	0.760		0.810	0.885	
	H		0.580	0.613	0.678		0.769	0.846	
Nilas (gray)	V		0.775	0.813	0.837		0.880	0.915	
	H		0.720	0.765	0.800		0.840	0.880	
Nilas (light)	V			0.910	0.950		0.960	0.955	
	H			0.850	0.890		0.930	0.925	
Densely packed 3-cm-thick pancakes	V	0.740	0.750	0.748	0.811	0.826	0.868	0.893	
	H	0.595		0.638	0.700	0.715	0.761	0.780	
First-year ice	V	0.935 [0.010]	0.900 (0.020)	0.924 (0.036)	0.941 (0.019)	0.960 (0.019)	0.955 (0.015)	0.926 (0.045)	0.934 (0.015)
	H	0.850 [0.065]	0.840 (0.025)	0.876 (0.021)	0.888 (0.019)	0.910 (0.020)	0.913 (0.013)	0.886 (0.031)	0.895 (0.009)
Dry multiyear	V	0.926 [0.037]	0.925 (0.020)	0.890 (0.035)	0.850 (0.068)	0.787 [0.080]	0.764 (0.079)	0.680 (0.105)	0.566 [0.061]
	H	0.865	0.820	0.817	0.780	0.635	0.706	0.650	0.535

Brightness temperatures – dependences on surface type, season and frequency

O = open water

F = First year ice

M = Multiyear ice

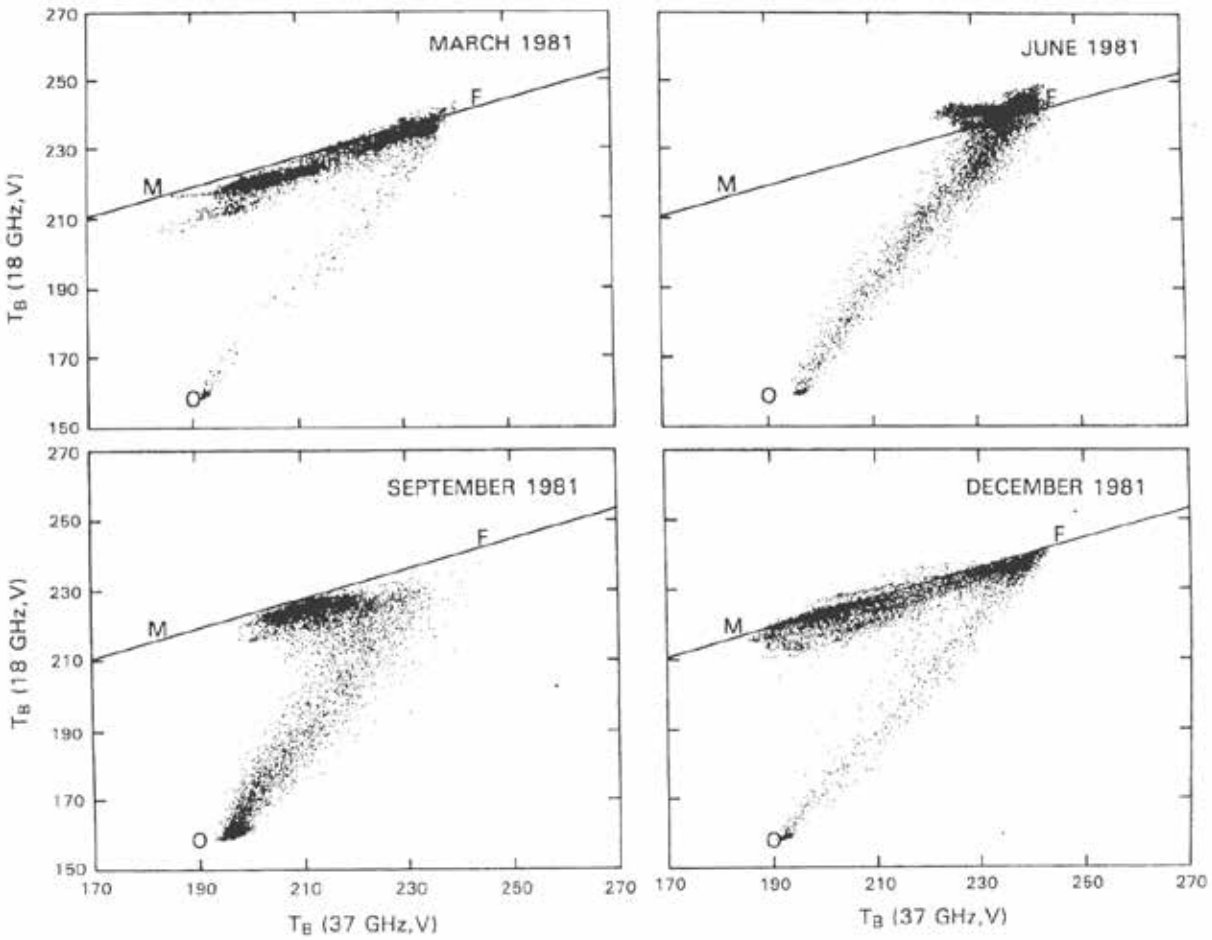

Figure 6. Scatterplots of 18 GHz(V) vs. 37 GHz(V) using SMMR data for March, June, September, and December 1981 [from Comiso, 1990].

3D scatter plots

O = open water

A = First-year ice

D = Multi-year ice

C, B, E = different ice conditions, including sub-pixel mixtures

W = Wet snow, or melt ponds on ice

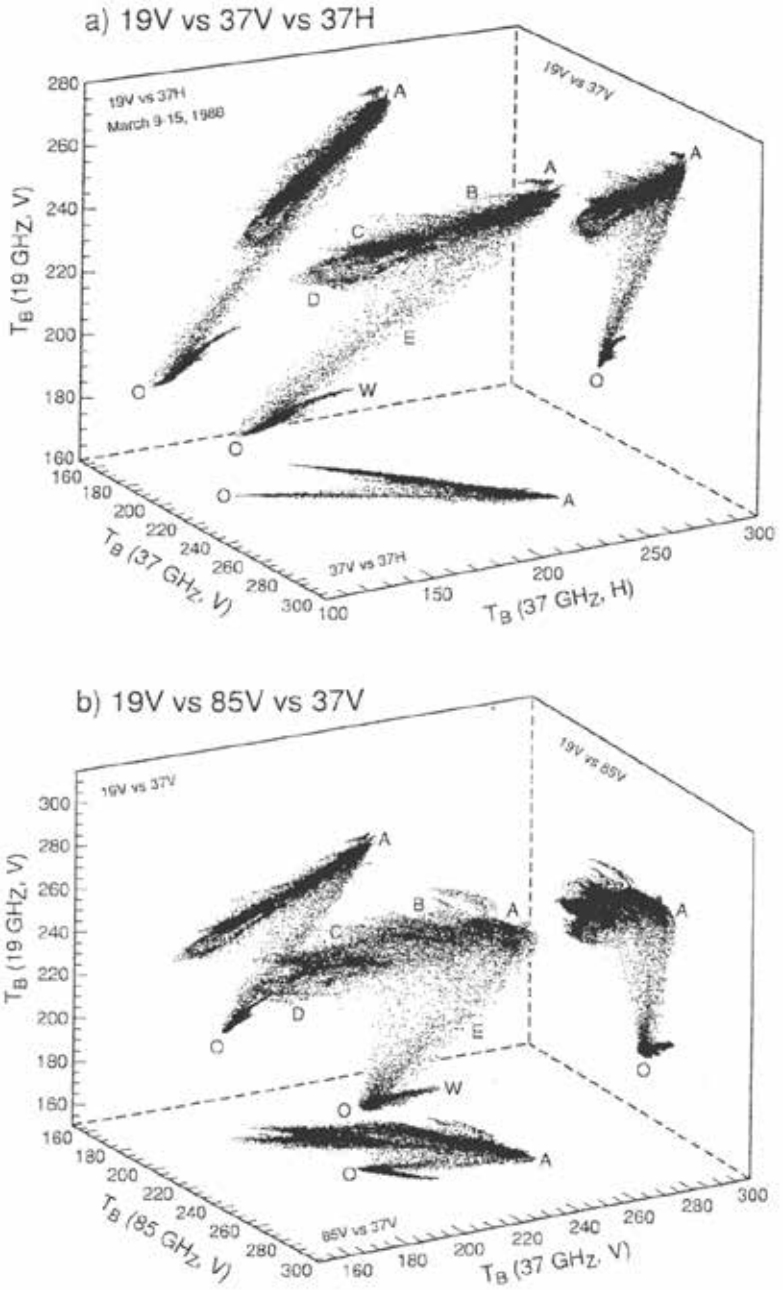

Figure 5. 3-D scatterplots of SSM/I brightness temperatures using: (a) 19 GHz(V) vs. 37 GHz(V) vs. 37 GHz(H) and (b) 19 GHz(V) vs. 85 GHz(V) vs. 37 GHz(V).

UNIVERSITY OF MIAMI
ROSENSTIEL
SCHOOL of MARINE &
ATMOSPHERIC SCIENCE

Spatial resolution

Spatial resolution in the microwave images relatively poor.

Generally oversampled to a higher resolution grid, typically 25 km or 6.25 km

Microwave data less influenced by clouds, and contain complementary information to the visible or infrared imagery.

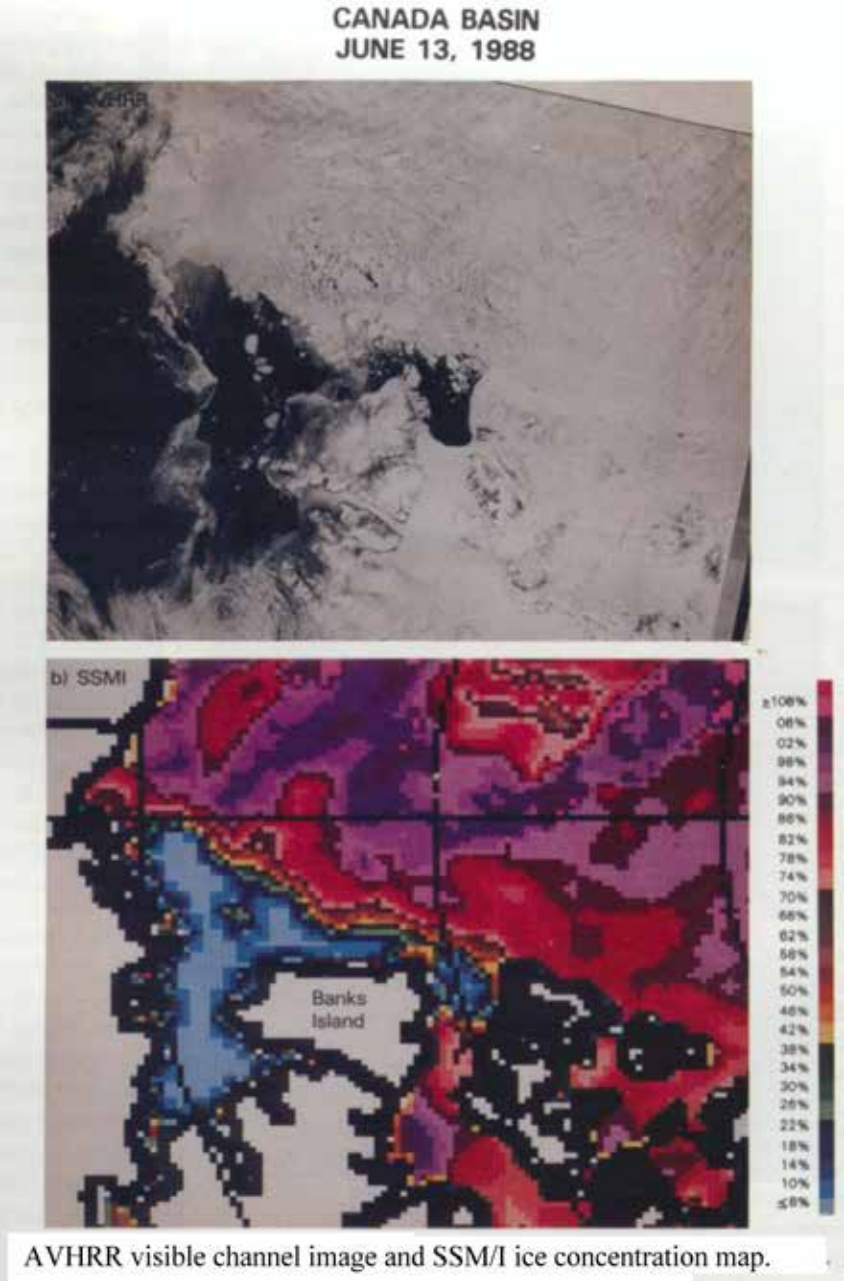

AVHRR visible channel image and SSM/I ice concentration map.

AMSR-E Arctic ice animations

From University of Bremen:

http://www.iup.uni-bremen.de:8084/amsr/#Animations

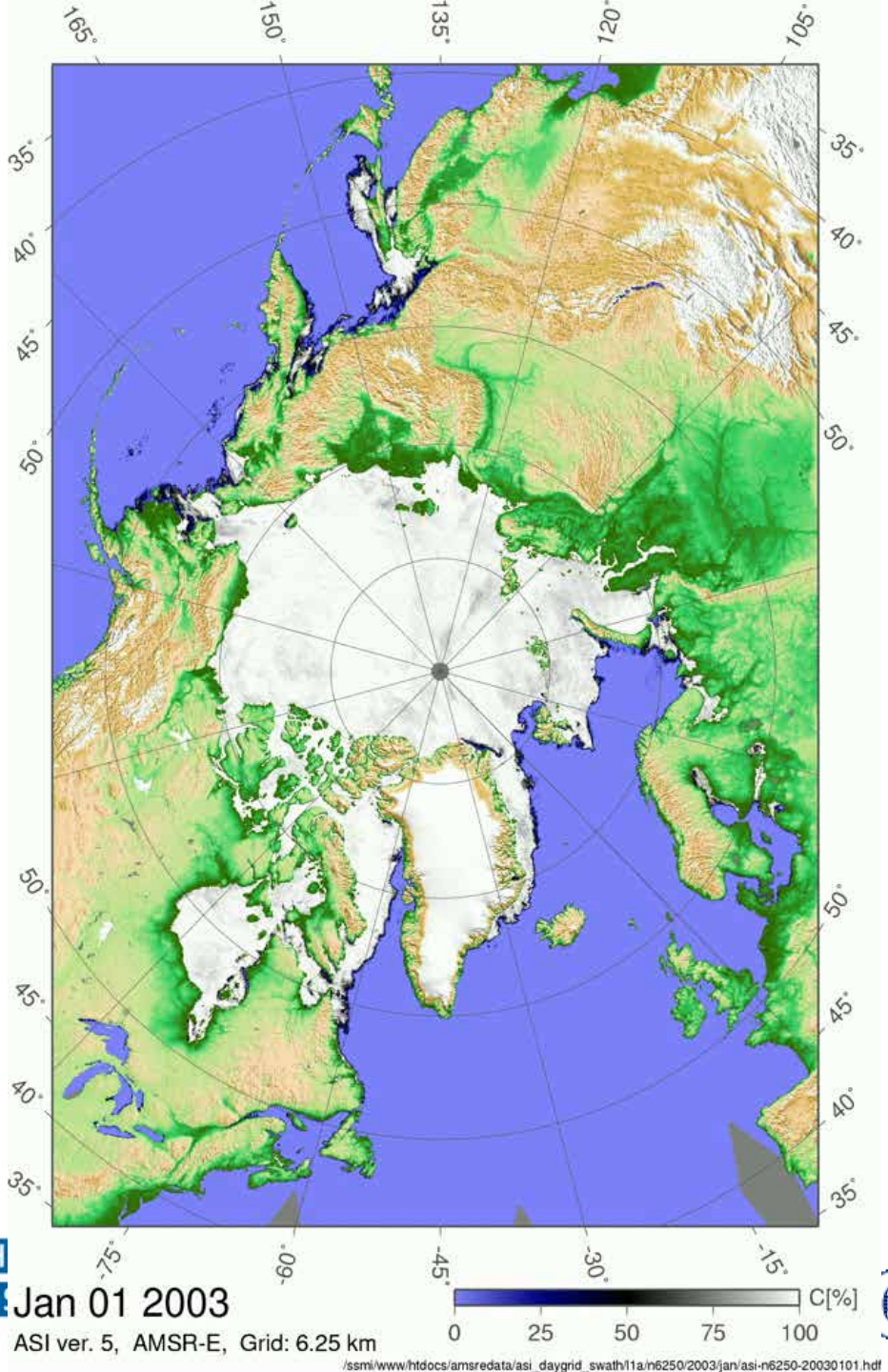

UNIVERSITY OF MIAMI
ROSENSTIEL SCHOOL of MARINE & ATMOSPHERIC SCIENCE

ESA EARTH ON EARTH

Arctic Sea Ice Time Series

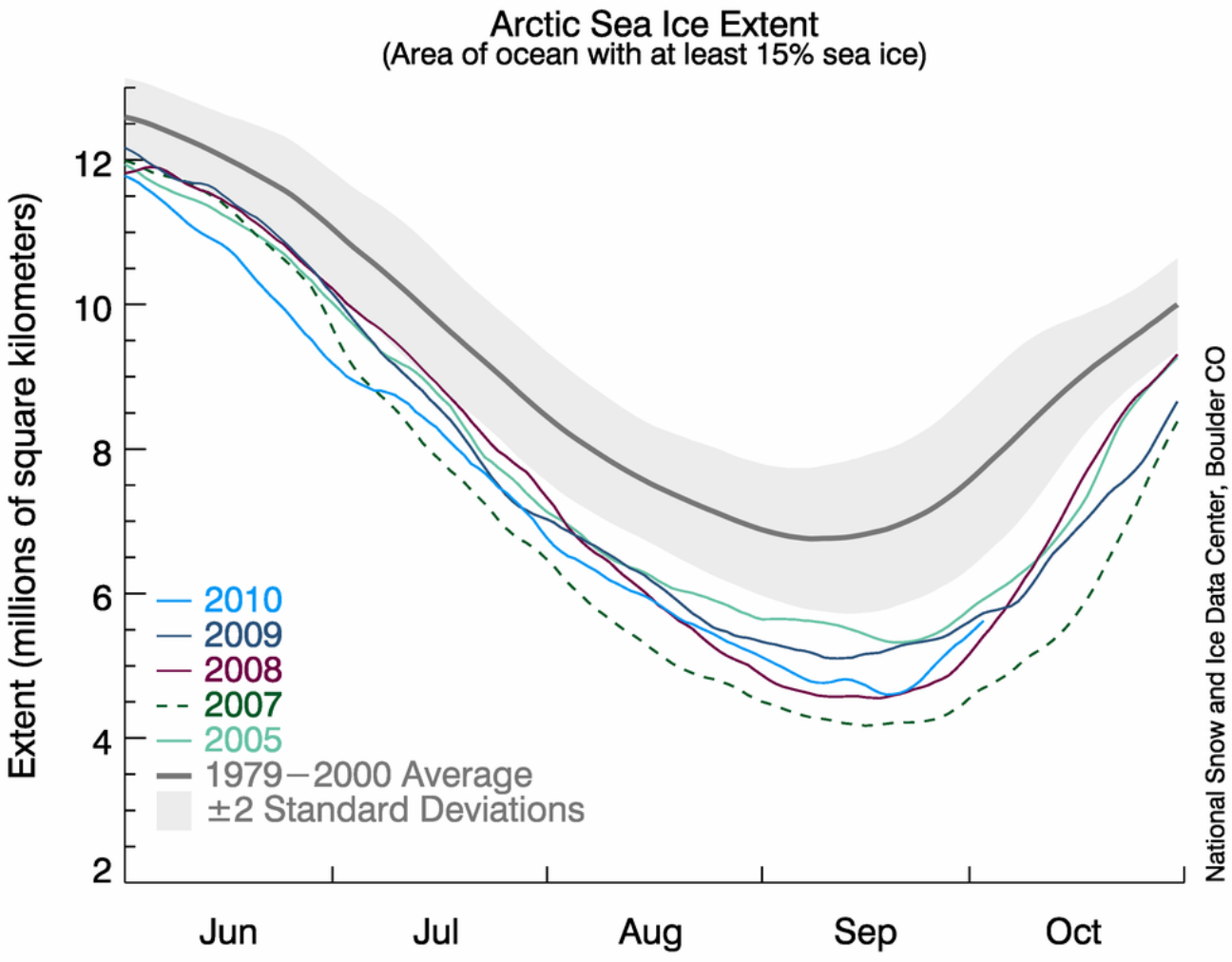

New minimum in 2011.

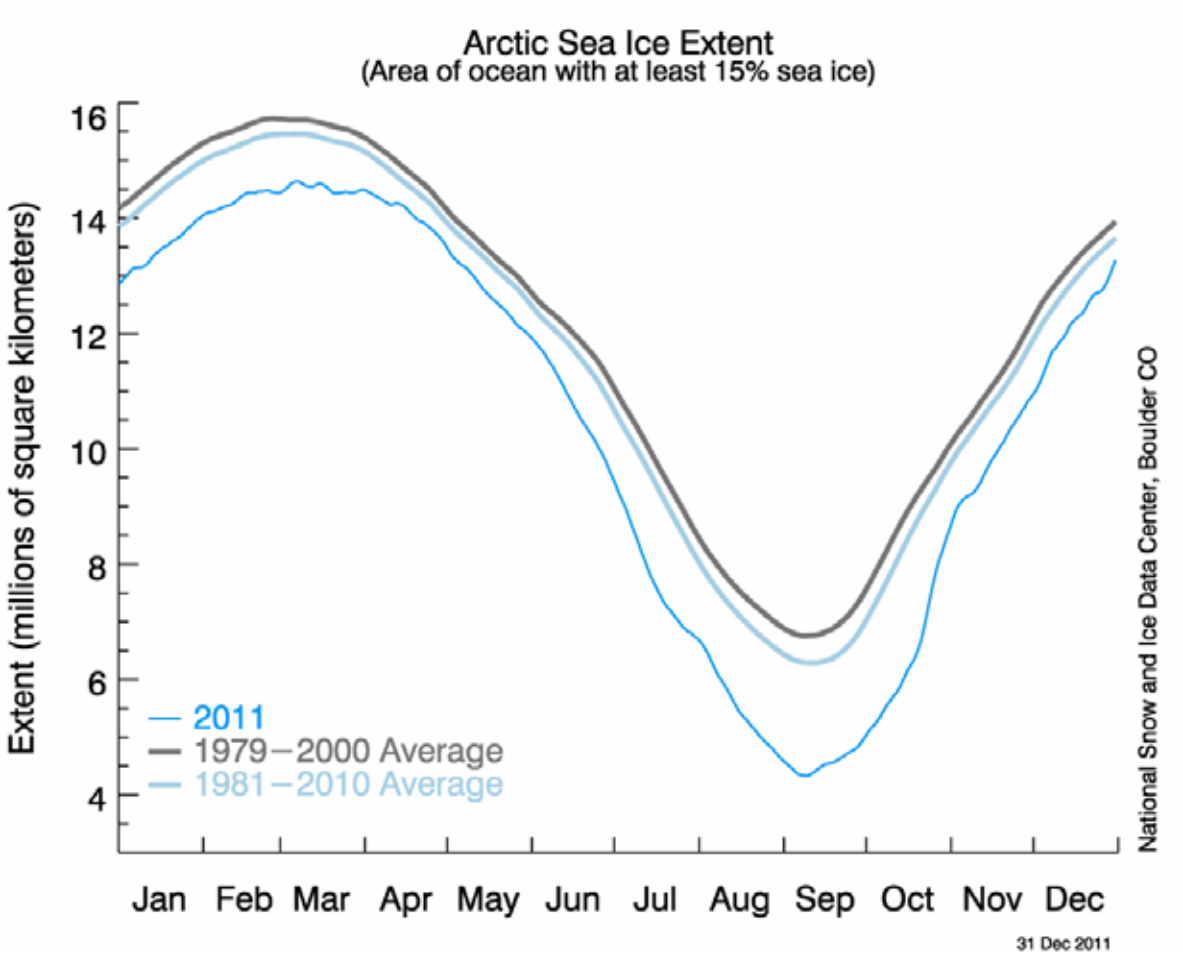

New minimum in 2012?

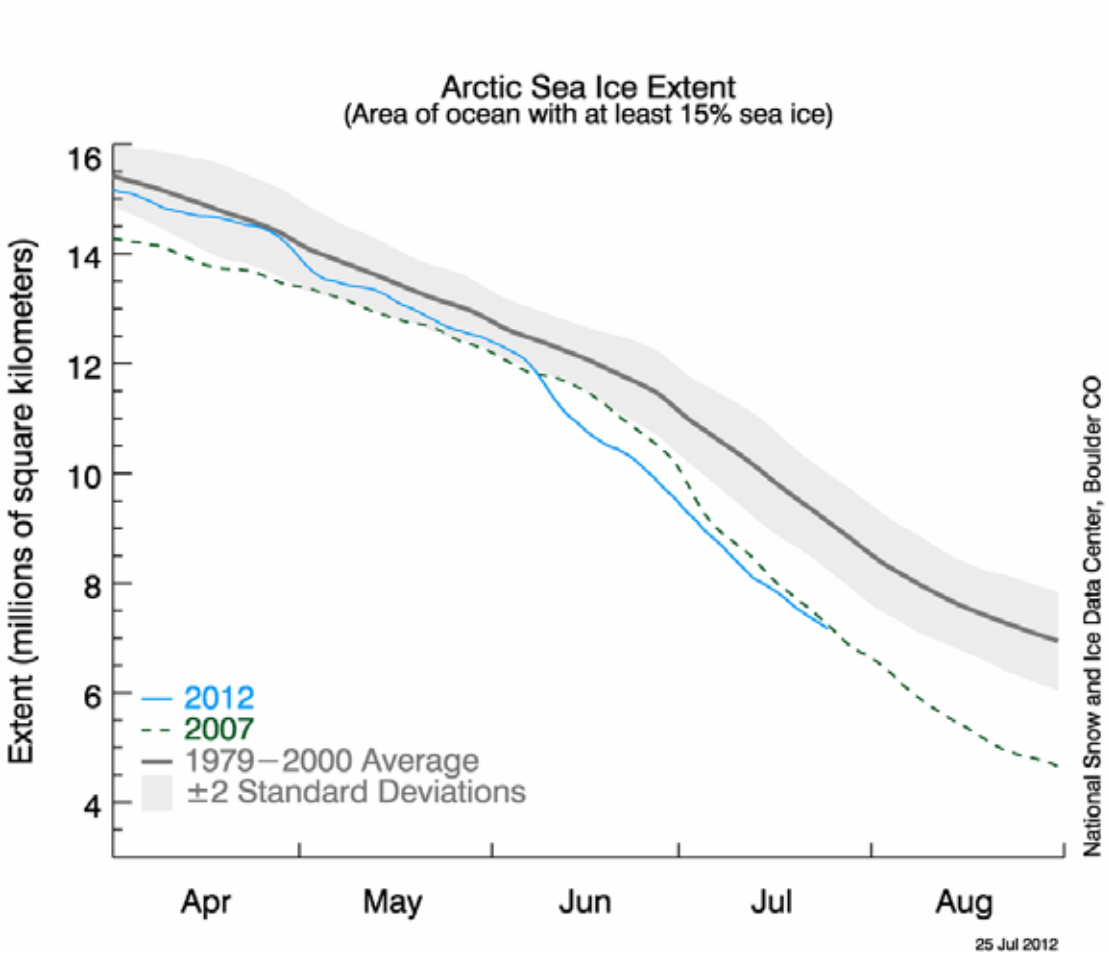

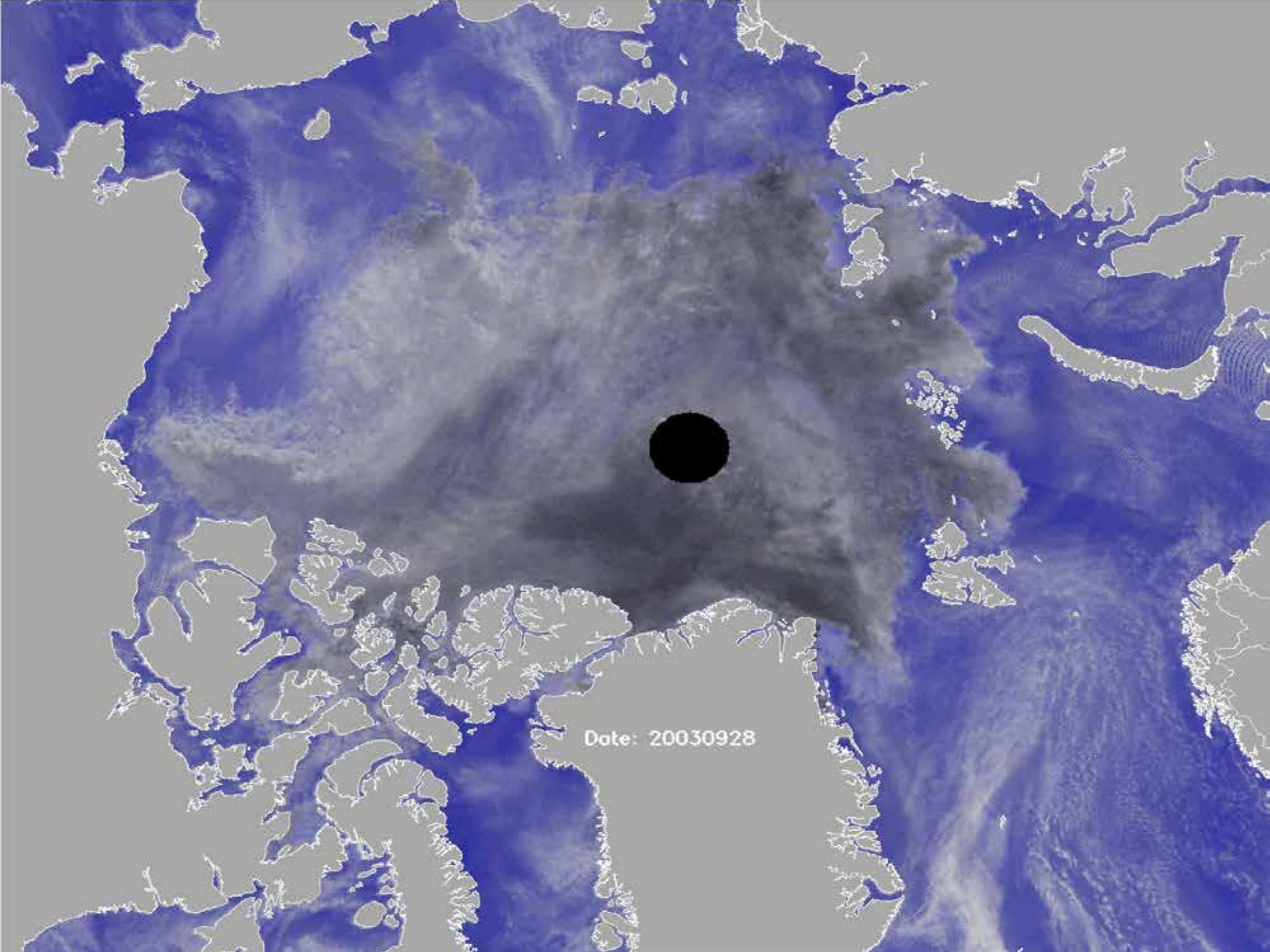
Date: 20030928

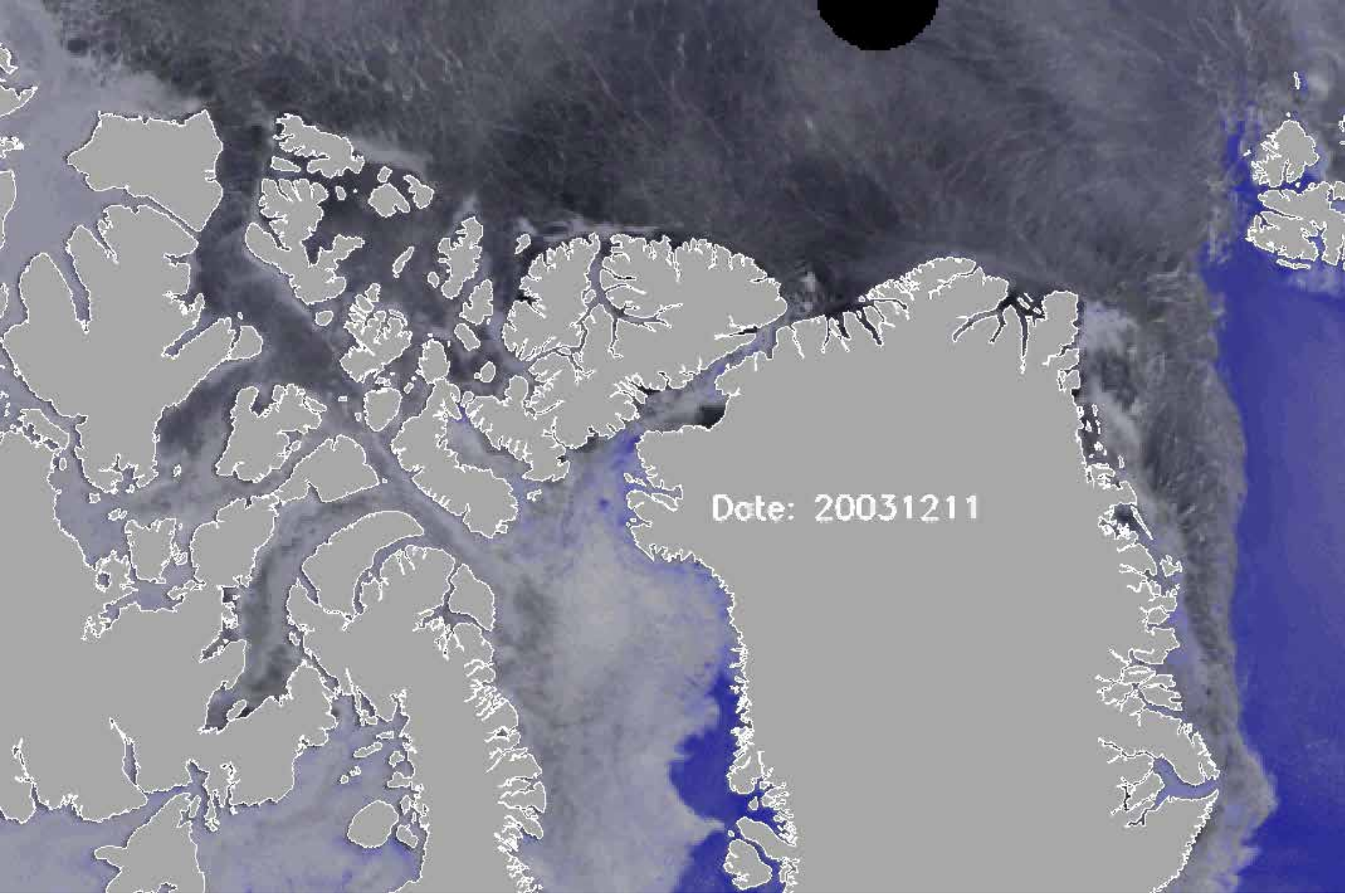
Date: 20031211

TRMM – Tropical Rainfall Measuring Mission

The Tropical Rainfall Measuring Mission (TRMM) is a joint mission between NASA and the Japan Aerospace Exploration Agency (JAXA) designed to monitor and study tropical rainfall. Launched 27 November 1997.

* Precipitation Radar (PR)

* TRMM Microwave Imager (TMI)

* Visible Infrared Radiometer (VIRS)

* Cloud and Earth Radiant Energy Sensor (CERES)

* Lightning Imaging Sensor (LIS)

http://trmm.gsfc.nasa.gov/

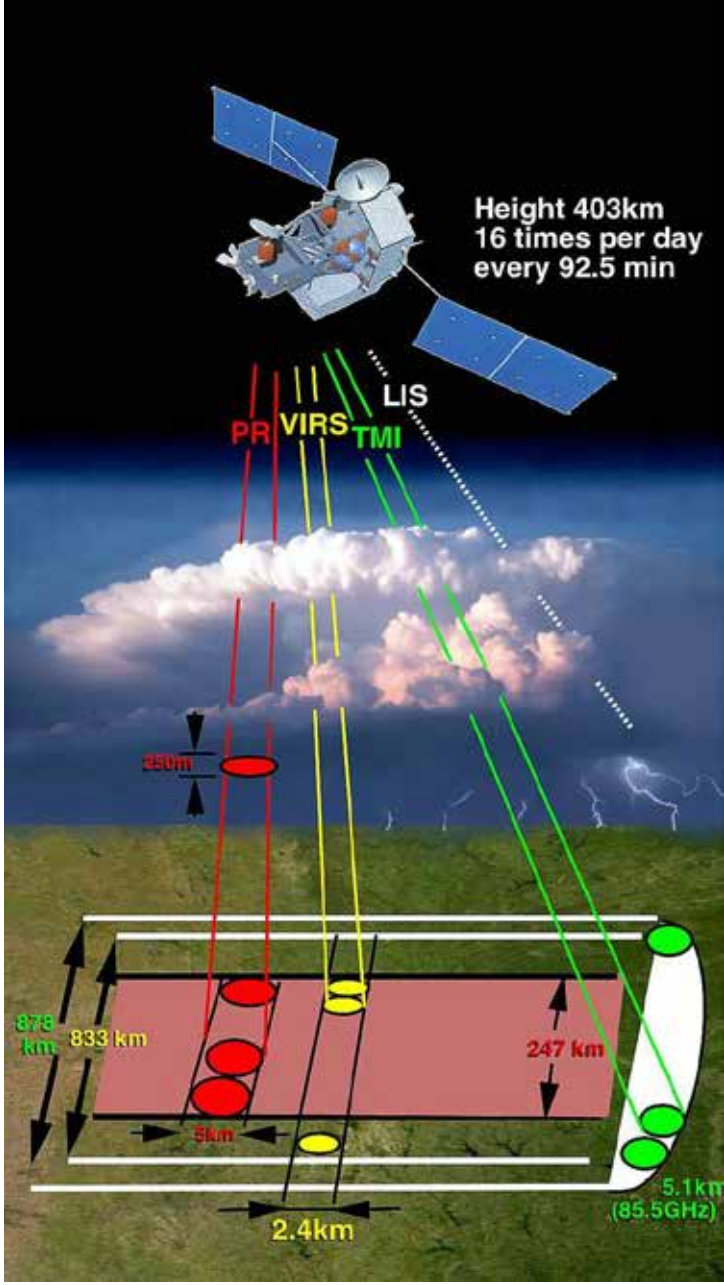

TRMM Microwave Imager

- Derived from SSM/I.
- The TMI measures the intensity of radiation at five separate frequencies: 10.7, 19.4, 21.3, 37, 85.5 GHz.
- 878 km swath.
- September 2001, the TMI orbit was boosted from an altitude of 350 km to 400 km.
- Errors in the knowledge of the satellite roll and pitch, particularly right after the 2001 orbit boost.
- Data from 40^{o}S to 40^{o}N.

TMI Sea Surface Temperatures

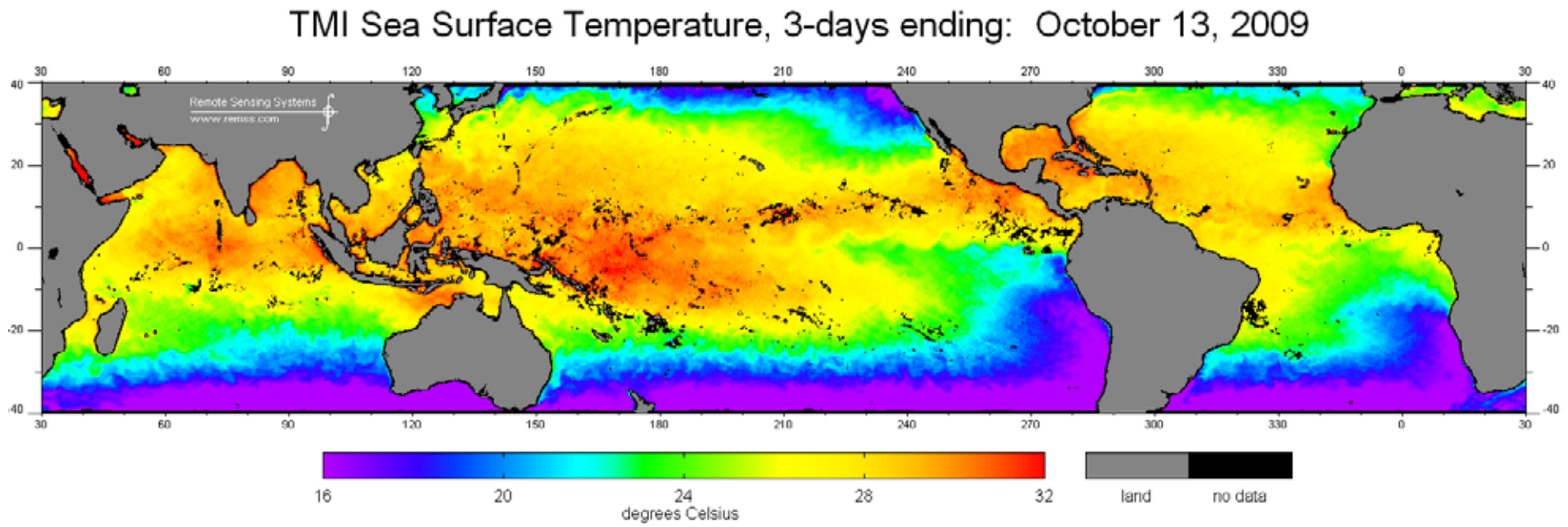

TMI has a 10.7 GHz channel which is sensitive to SST in warm water.

http://www.remss.com/tmi/tmi_3day.html

AMSR-E on EOS-Aqua

AMSR-E

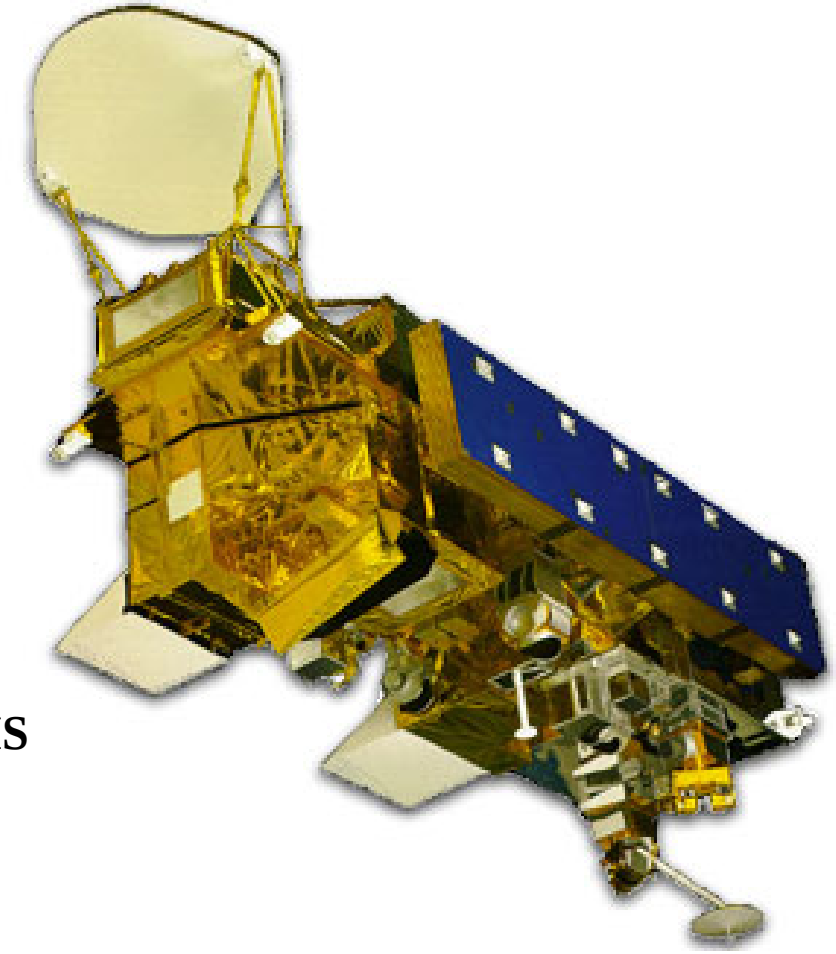

MODIS

Aqua launched 4 May 2002, terminated on October 4, 2011.

Low frequency SST sensitivity means very large antenna is needed for even moderate surface resolution.

Offset parabolic reflector, 1.6 m in diameter, and rotating drum at 40 rpm

But side lobe contamination is a significant issue, especially in coastal regions.

http://aqua.nasa.gov/

http://aqua.nasa.gov/about/instrument_amsr.php

AMSR-E: Advanced Microwave Scanning Radiometer for EOS.

Table 1. AMSR-E PERFORMANCE CHARACTERISTICS						
CENTER FREQUENCIES (GHz)	**6.925**	**10.65**	**18.7**	**23.8**	**36.5**	**89.0**
BANDWIDTH (MHz)	350	100	200	400	1000	3000
SENSITIVITY (K)	0.3	0.6	0.6	0.6	0.6	1.1
MEAN SPATIAL RESOLUTION (km)	56	38	21	24	12	5.4
IFOV (km x km)	74 x 43	51 x 30	27 x 16	31 x 18	14 x 8	6 x 4
SAMPLING RATE (km x km)	10 x 10	10 x 10	10 x 10	10 x 10	10 x 10	5 x 5
INTEGRATION TIME (MSEC)	2.6	2.6	2.6	2.6	2.6	1.3
MAIN BEAM EFFICIENCY (%)	95.3	95.0	96.3	96.4	95.3	96.0
BEAMWIDTH (degrees)	2.2	1.4	0.8	0.9	0.4	0.18

http://www.ghcc.msfc.nasa.gov/AMSR/

Microwave SSTs

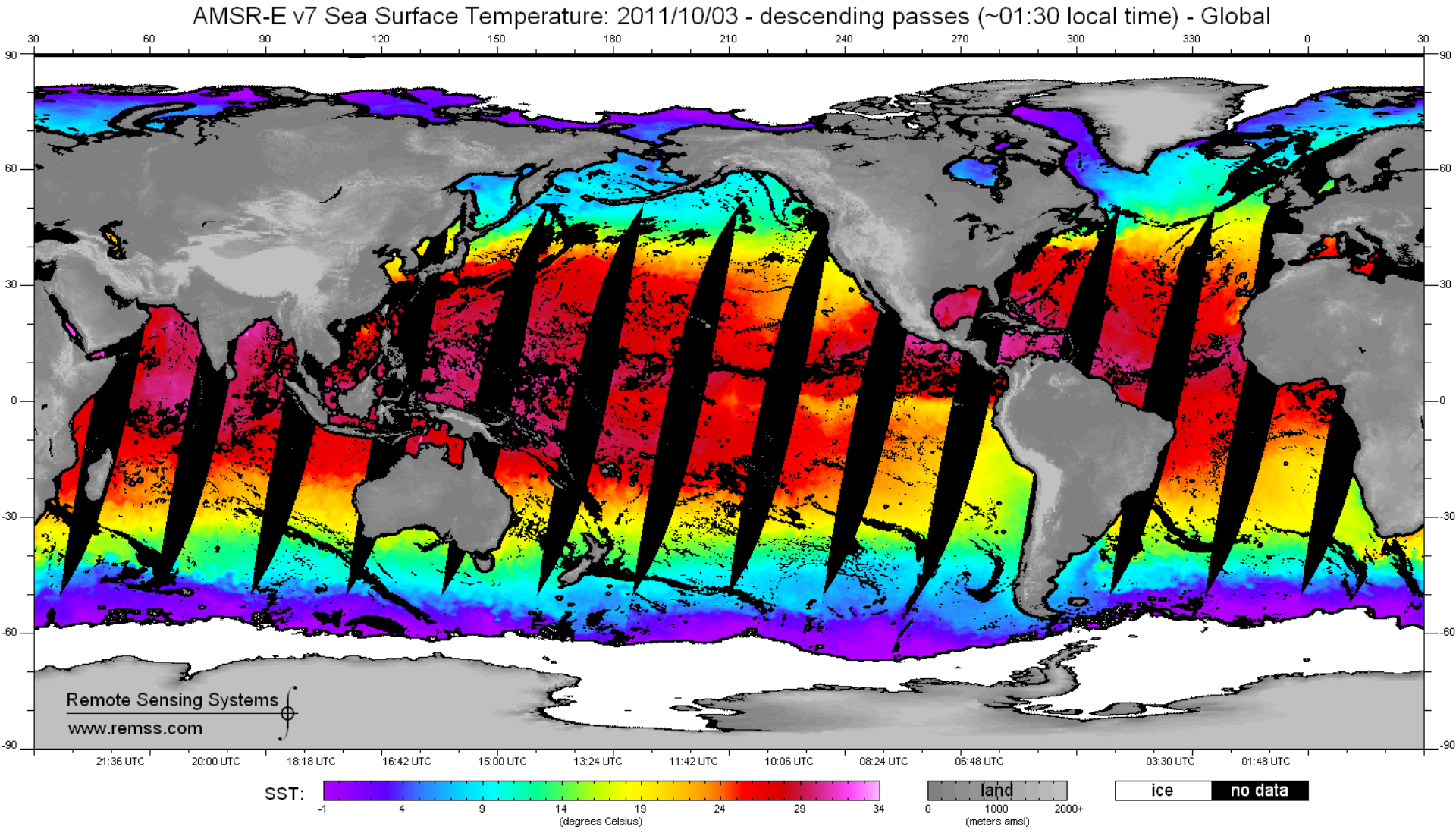

Global microwave SSTs

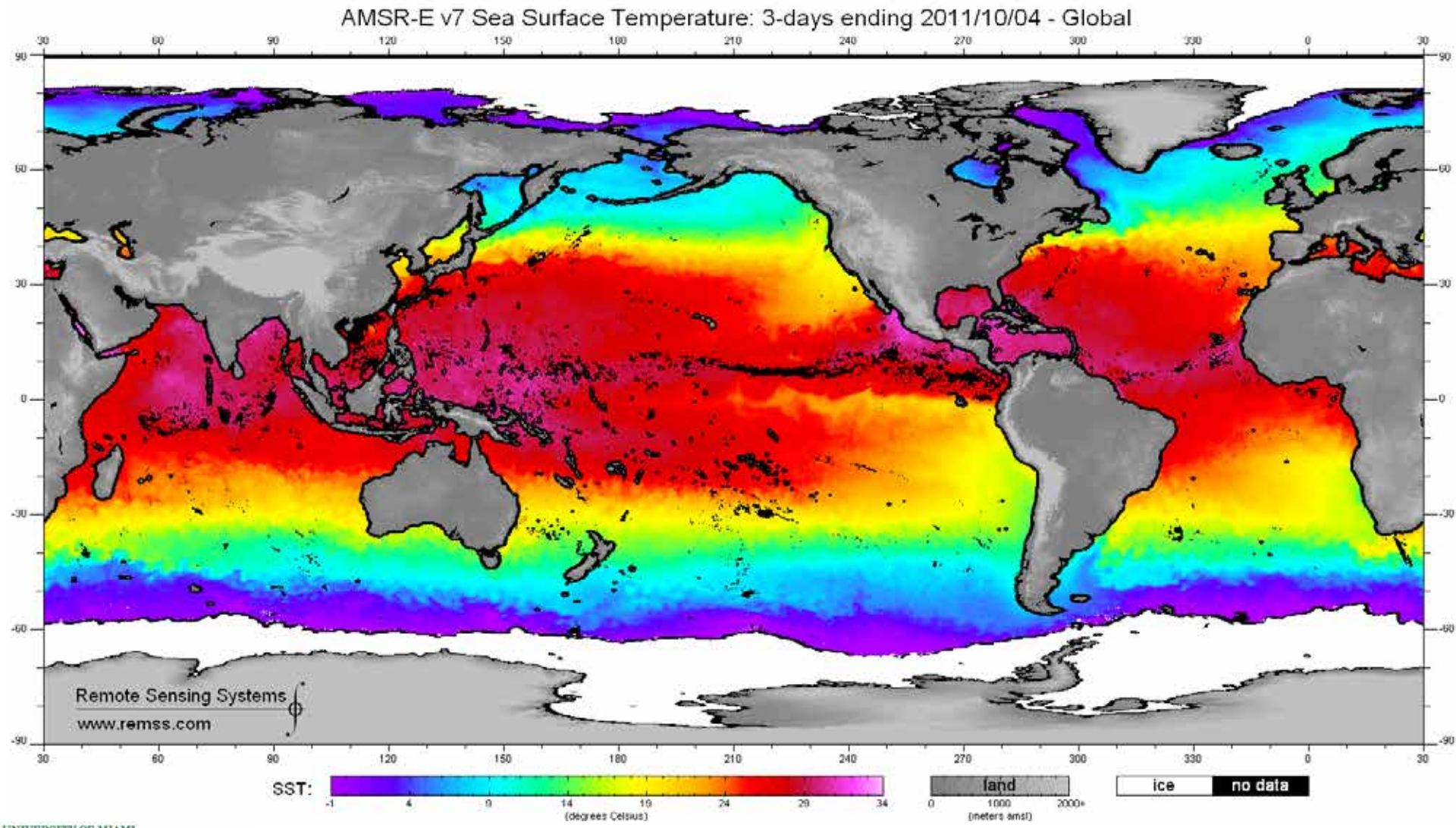

AMSR-E SST

Loop from Remote Sensing Systems http://www.remss.com/

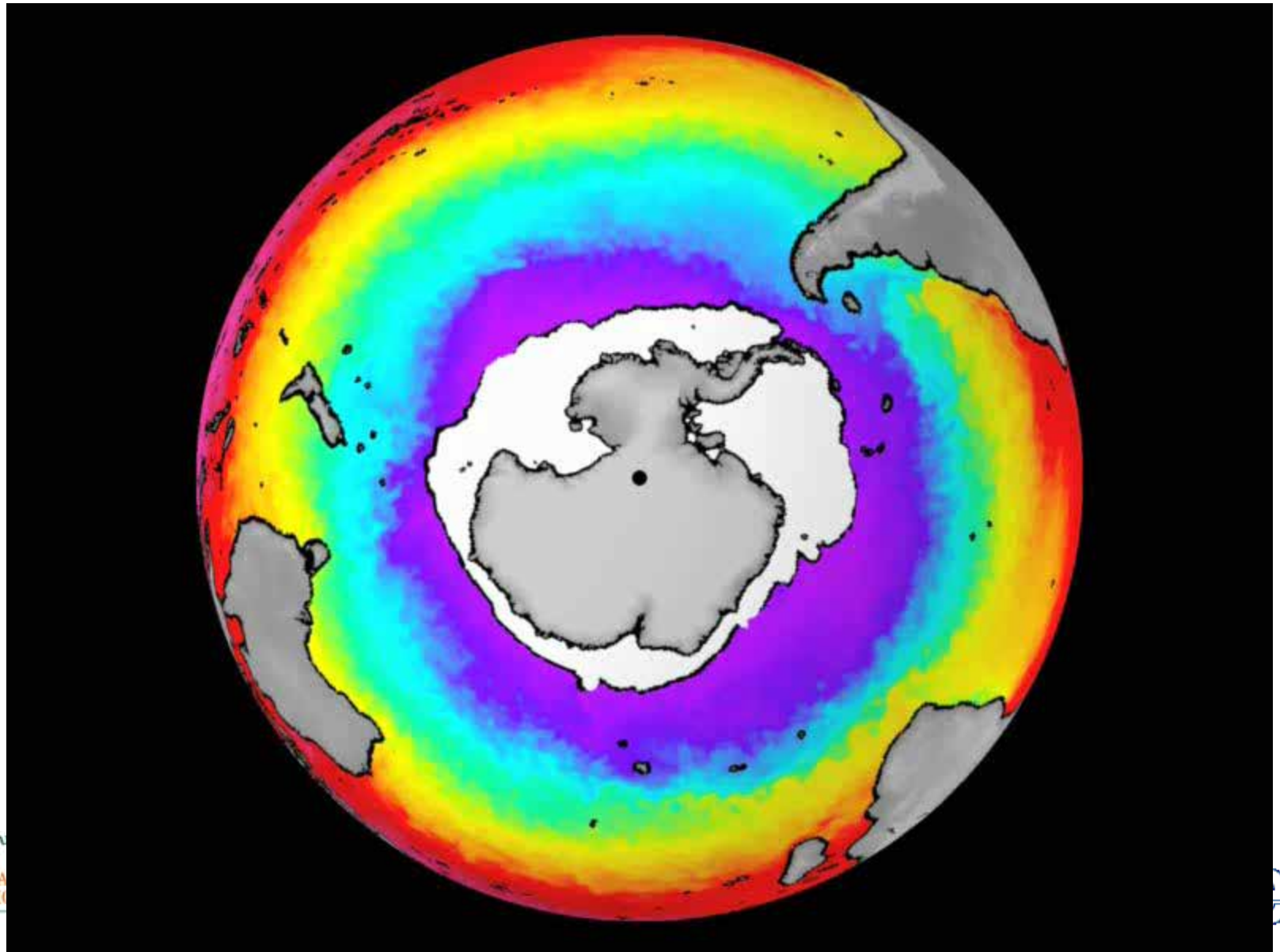

TMI microwave SST

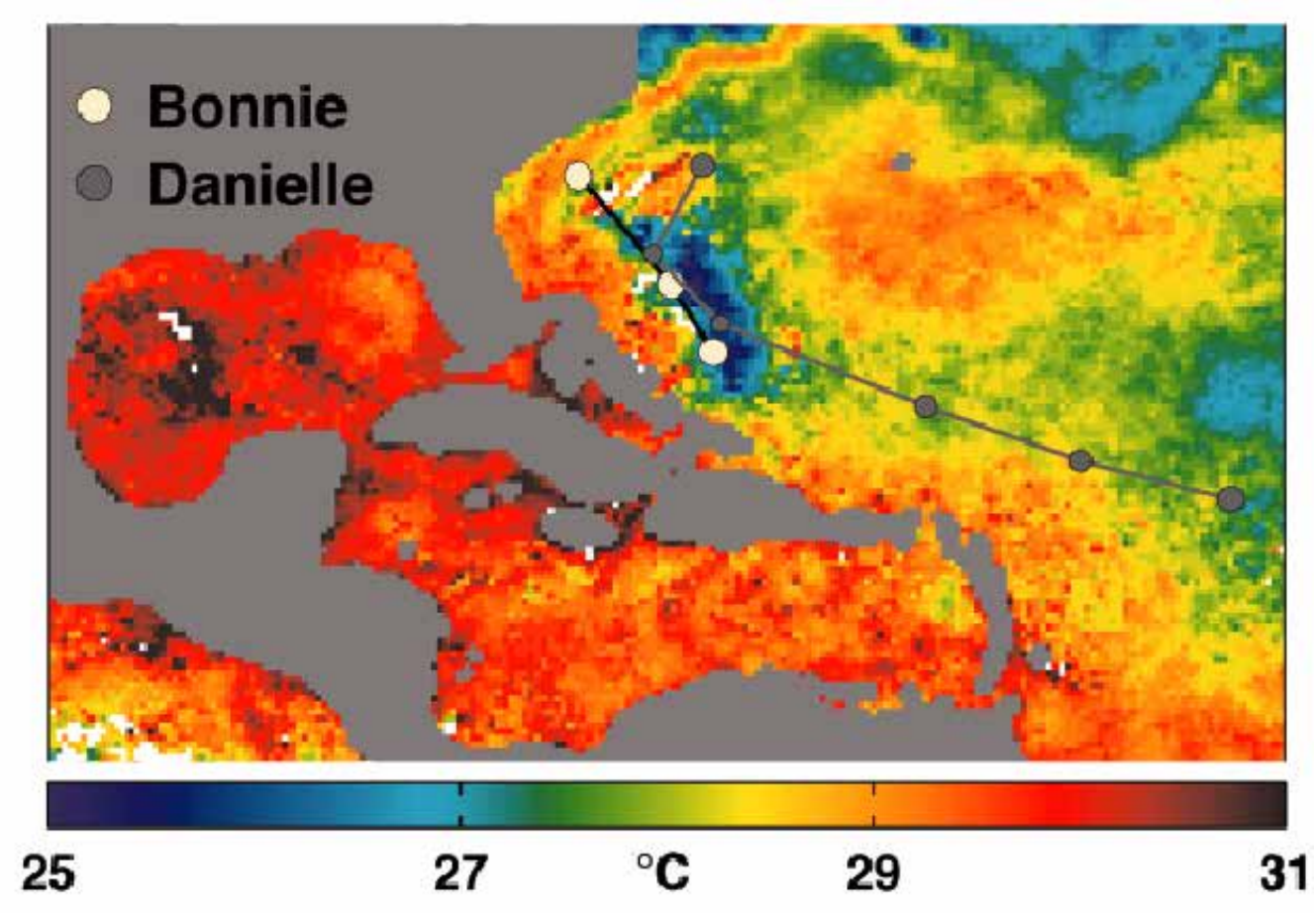

From: Wentz, F.J., C. Gentemann, D. Smith and D. Chelton, 2000. Satellite measurements of sea-surface temperature through clouds. Science, 288: 847-850.

Blending of infrared and microwave SSTs

AMSR-E MODIS 10km OI SST

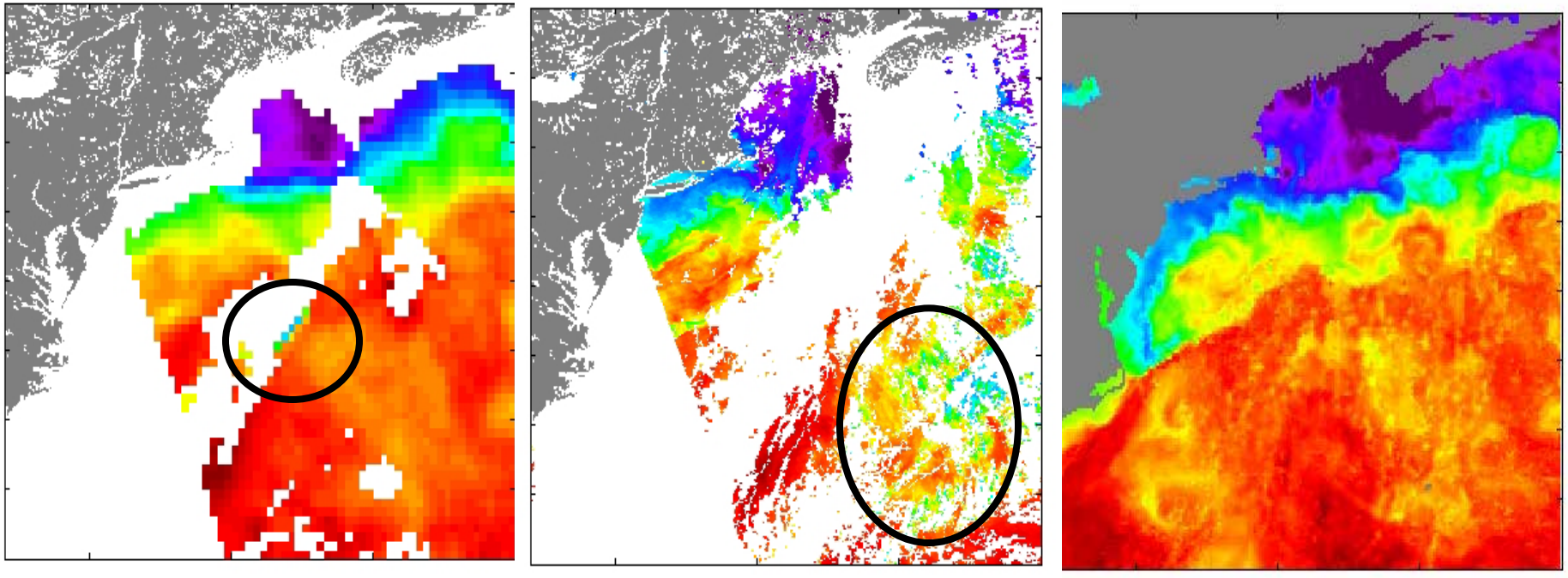

From Chelle Gentemann

AMSR-2 on GCOM-W1

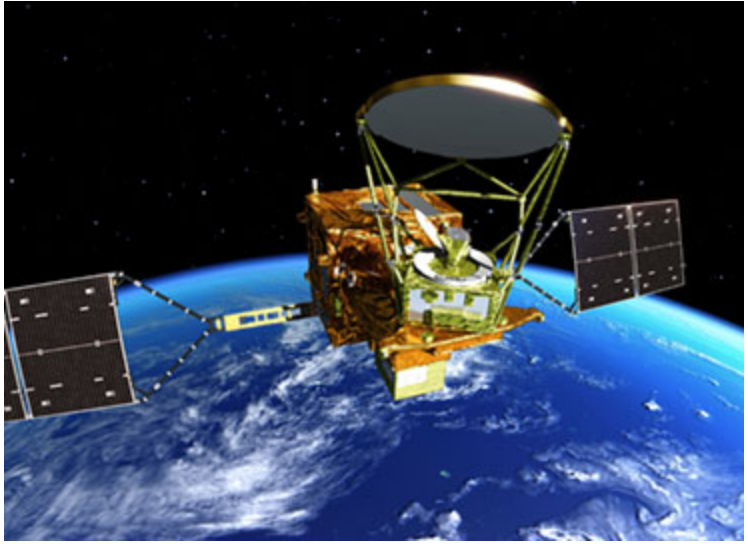

GCOM-W1/Main Specifications of AMSR2

Scan and rate	Conical scan at 40 rpm
Antenna	Offset parabola with 2.0m dia.
Swath width	1450km
Incidence angle	Nominal 55 degrees
Digitization	12bits
Dynamic range	2.7-340K
Polarization	Vertical and horizontal

AMSR2 Channel Set

Center Freq.	Band width	Pol.	Beam width	Ground res.	Sampling interval
GHz	MHz		degree	km	km
6.925/7.3	350	V/H	1.8	35 x 62	10
10.65	100		1.2	24 x 42	
18.7	200		0.65	14 x 22	
23.8	400		0.75	15 x 26	
36.5	1000		0.35	7 x 12	
89.0	3000		0.15	3 x 5	5

UNIVERSITY OF MIAMI
ROSENSTIEL
SCHOOL of MARINE &
ATMOSPHERIC SCIENCE

ESA EARTH
ON EARTH

AMSR-2 data

第一期水循環変動観測衛星「しずく」
Global Change Observation Mission 1st-Water "SHIZUKU"

AMSR2 による地球全体の擬似カラー合成画像
Color composite image of global Earth by AMSR2

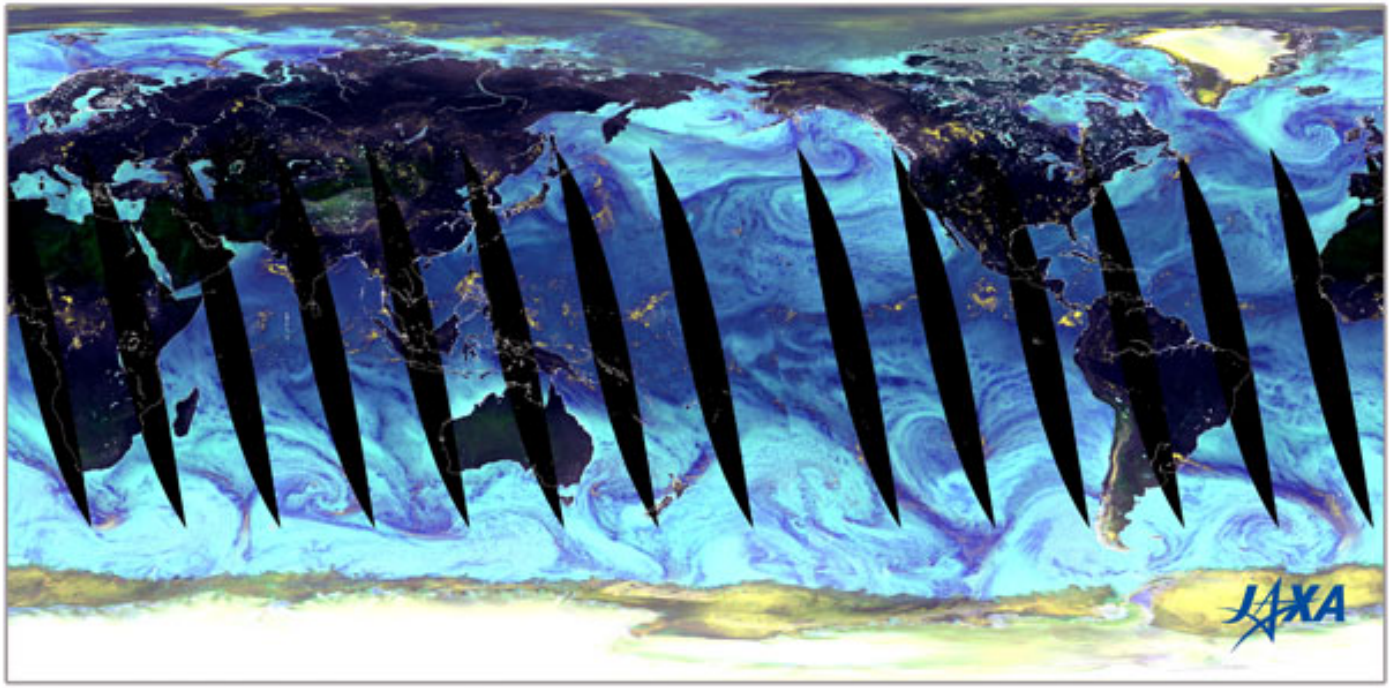

図は、平成24年7月3日午前9時頃から7月4日午前9時頃(日本時間)にかけての約1日間に、「しずく」搭載のAMSR2が地球の全体を観測した擬似カラー合成画像で、89.0GHz垂直・水平偏波、23.8GHz垂直偏波の輝度温度を使用しています。

Figure is one-day color composite image of global Earth by the AMSR2 on-board the SHIZUKU on July 3, 2012 (UTC). Brightness temperatures of 89.0-GHz (both vertical and horizontal polarization) and 23.8-GHz (vertical polarization) channels were used.

GCOM JAXA

http://suzaku.eorc.jaxa.jp/GCOM_W/w_amsr2/whats_amsr2.html

AMSR-2 Arctic Sea Ice

第一期水循環変動観測衛星「しずく」
Global Change Observation Mission 1st-Water "SHIZUKU"

AMSR2 による北極域の海氷分布
Distribution of Arctic sea ice concentration by AMSR2

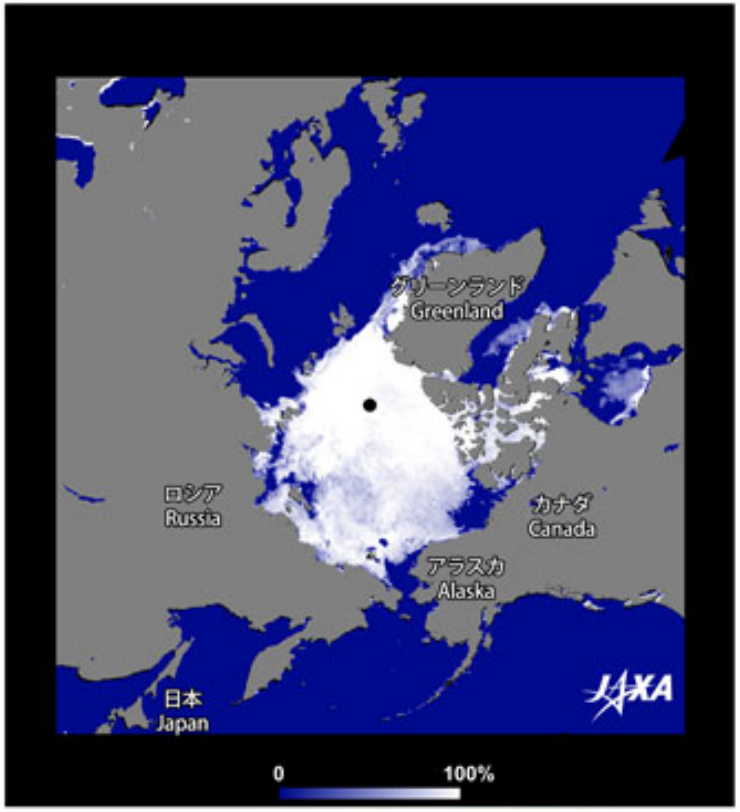

図は、平成24年7月3日午前8時頃～4日午前9時頃（日本時間）の北極海の海氷分布図です。「しずく」は極地方上空を100分に1回通過するため、北極海全体を毎日観測することが可能です。白色が濃い領域は海氷に覆われていることを示し、海は青色、陸地は灰色、観測されていない領域は黒色で表されています。近年北極海航路が注目されていますが、ロシア沿岸を航行する北東航路、およびカナダ・アラスカ沿岸を航行する北西航路のいずれについても、すでに一部の海域で海氷がなくなっている様子が捉えられています。

Figure shows the distribution of sea ice concentration from 8:00 a.m. on July 3 to 9:00 a.m. on July 4, 2012 (JST). Since the SHIZUKU flies over polar regions every 100 minutes, the entire area of the Arctic Ocean can be observed daily. Colors from white to blue indicate the sea ice concentration. Areas of ocean, land, and no-observations are indicated by blue, gray, and black colors. The Arctic sea routes are getting a lot of attention during recent years. Along both the Northeast Passage and the Northwest Passage, which are running along the Russian Arctic coast and the northern coast of the North America, respectively, some sea areas are already free of sea ice.

GCOM JAXA

The A-Train

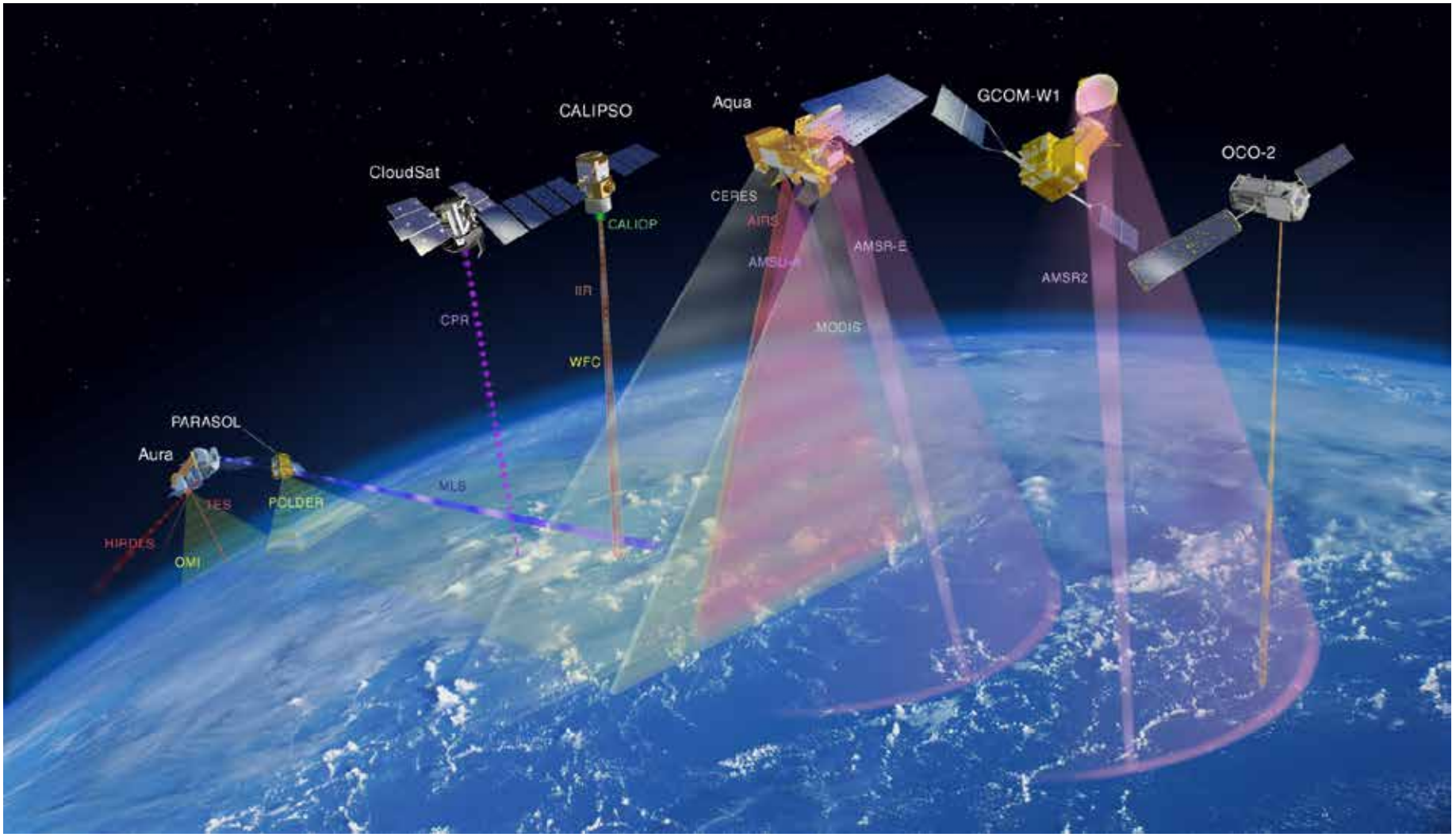
CALIPSO
Aqua
GCOM-W1
OCO-2
CloudSat
CERES
CALIOP
AIRS
AMSR-E
AMSU-A
AMSR2
IIR
CPR
MODIS
WFC
PARASOL
Aura
MLS
TES
POLDER
HIRDES
OMI

Aquarius

- Aquarius is a focused satellite mission to measure global Sea Surface Salinity (SSS). Scientific progress is limited because conventional in situ SSS sampling is too sparse to give the global view of salinity variability that only a satellite can provide.
- Aquarius will resolve missing physical processes that link the water cycle, the climate, and the ocean.
- Launched June 10, 2011.

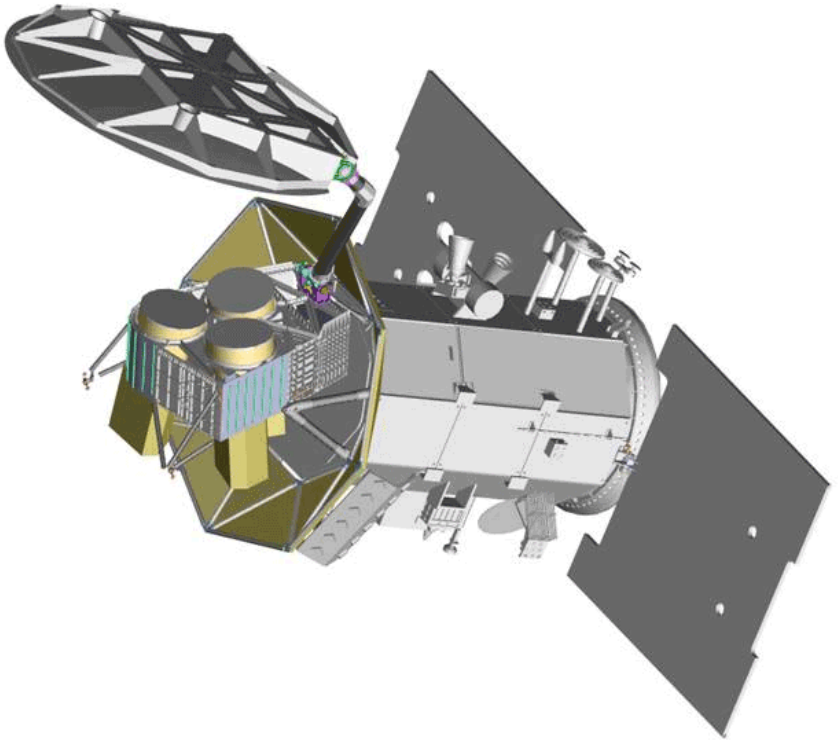

http://aquarius.nasa.gov/

Aquarius specifications

Item Value	Summary/Units
Sensor type	Radiometers at 1.413 GHz Scatterometer at 1.26 GHz
Number of instruments	1
Number of channels	3 antenna feeds, 3 polarimetric radiometers, 1 polarimetric scatterometer
Size	3 m x 6 m_ 4 m, antenna deployed
Mass with contingency	400 kg
Power with contingency	450 W, 100% duty cycle, 50 W standby
Data rate with contingency	TBD kbps
Optical layout	3 antenna beams at 29°, 38°, 45° incidence angles to shadow side of orbit
Footprint sizes	76 X 94 km, 84 X 120 km, 96 X 156 km
Radiometer NEDT 6 sec integration	0.08 K
Radiometer stability for 7 days	0.12 K
Radar calibration stability for 7 days	0.13 dB
Ground calibration scheme	In situ SSS sensors on buoys and ships
Onorbit calibration scheme	Noise diodes in radiometer and cold sky measurements
Pointing requirements (3s)	0.05 (knowledge); 0.5 (control and stability)
Command and control requirements	Once per month for cold sky measurement
Operational modes	ON, Standby, Survival

Aquarius – SAC-D

AQUARIUS

Observatory Illustration

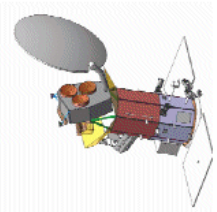

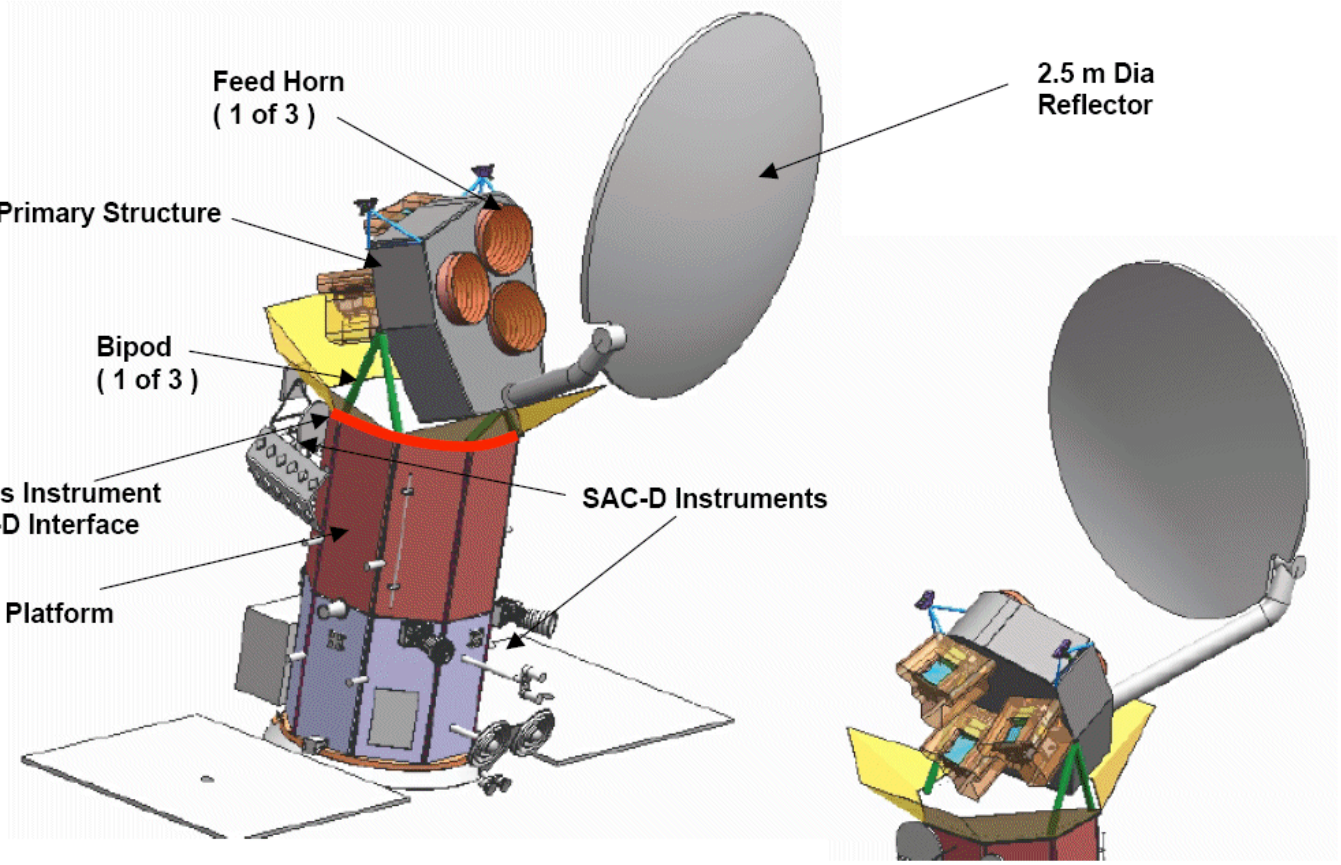

Aquarius Instrument 1

AQUARIUS

Instrument Summary 1

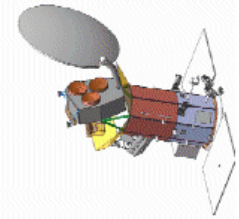

KEY ORBIT PARAMETERS

Parameter	*Value*	
Observatory Orbit Altitude (km)	657	(655-685 km)
Orbit Inclination (deg)	98.0	(sun-synchronous)
Orbit Equatorial Crossing	6:00 PM ascending	
Ground-track repeat interval	7 days, 103 orbits	

KEY INSTRUMENT PARAMETERS

Parameter	*Radiometer*	*Scatterometer*
Frequency (MHz)	~1413	1260
Band Width (MHz)	≤ 26	4
Swath Width (km)	407	373
Polarization	Th, Tv, T+45, T-45	HH, HV, VV, VH
PRF (Hz)	100	100
No. Measurements Per Second	58.3	5.6
Transmitter Power (W)		200 - 250
Transmit Pulse Length (ms)		1
Pulse Integration Time (ms)	~9	~1.6
A/D (# bits)		12
Data Rate (kbits/sec)	11.0	2.1
Measurement Integration Time (s)	6	6
Dynamic Range (K, σ_0)	<5 K to 1400 K	0 dB to -40 dB

Key Parameters
6/20/05

Aquarius Instrument 2

AQUARIUS

Instrument Summary 2

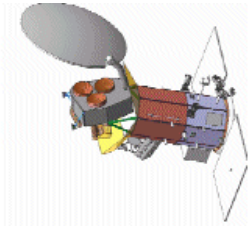

KEY ANTENNA PARAMETERS

Parameter	Value
Antenna	2.5 m diameter, offset parabola (2.5 x 2.9 linear dimension)
Feedhorns	3 feeds, 50 cm diam, equilateral triangle about focus

(off-nadir pointing angle of 33°)

	Radiometer			Scatterometer		
Parameter	Inner beam	Middle beam	Outer beam	Inner beam	Middle beam	Outer beam
Look Angle (deg)	25.8	33.8	40.3	25.9	33.9	40.3
Azimuth Angle (deg)	9.8	-15.3	6.5	9.7	-15.3	6.5
Average 3 dB Beam Width (deg)	6.1	6.3	6.6	6.5 / 4.7 *	6.7 / 4.8 *	7.1 / 5.1 *
Beam Efficiency (%)	94.0	92.4	90.4	89.9	87.6	85.4
Peak Gain (dBi)	29.1	28.8	28.5	28.5	28.1	27.7
Gain Stability (K, dB)	0.11	0.11	0.11	0.04	0.04	0.04
Peak Cross-Pole Gain (dBi)	6.5	8.6	10.3	6.3	8.4	10.1

* one-way / two-way 3 dB beam widths

KEY MEASUREMENT PARAMETERS/REQUIREMENTS

	Radiometer			Scatterometer		
Parameter	Inner beam	Middle beam	Outer beam	Inner beam	Middle beam	Outer beam
Incidence Angle (deg)	28.7	37.8	45.6	28.8	37.9	45.5
Footprint Size (3 dB one-way, two-way)	94 x 76	120 x 84	156 x 97	71 x 58	91 x 65	122 x 74
Noise-Equivalent Sigma-0 (dB, pulse)				-29	-26	-24
Stability (K, dB)	0.12	0.12	0.12	0.13	0.13	0.13
Radar Sensitivity (dB)				0.04	0.06	0.1
Radiometer Sensitivity (NEDT, K)	0.06	0.06	0.06			
Power Sensitivity (after integration) (dBm)	-137	-137	-137	-119	-126	-127

Note for reference: 0.1 K error for a 100 K T_B = 0.1 % => 0.004 dB error

Aquarius Overview

AQUARIUS

Selected Instrument Concept

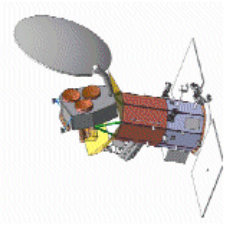

- Antenna
  - Radiometer & Scatterometer share feed and reflector (one antenna subsystem)
  - ≥ 2.5 m reflector diameter
  - Three feeds, in triangular geometry
  - Offset parabolic geometry
  - Three footprints in mechanically stable pushbroom configuration
- Radiometer
  - Radiometer ~27 MHz wide band centered at ~1413 MHz
  - Polarimetric radiometer (TH, TV, U (T+45°,T-45°)) for correcting for Faraday rotation
- Scatterometer
  - L-band, in space-radar band
  - Polarimetric (co-pol and cross-pol) for Faraday rotation correction and algorithm improvement
- ICDS (control and data system)
  - On-board storage, data processing
  - Interface with Service Platform

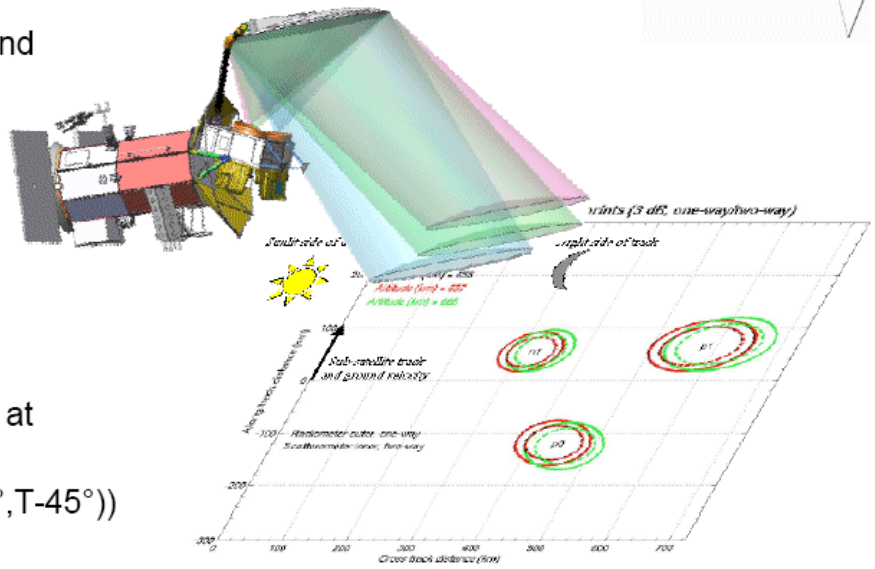

- Other
  - 3-year lifetime, single-string
  - 98 minute, sun-synchronous, 6 pm ascending orbit, 657 km equatorial altitude (655 km minimum, 685 km maximum over the orbit)

Aquarius Sea-Surface Salinity

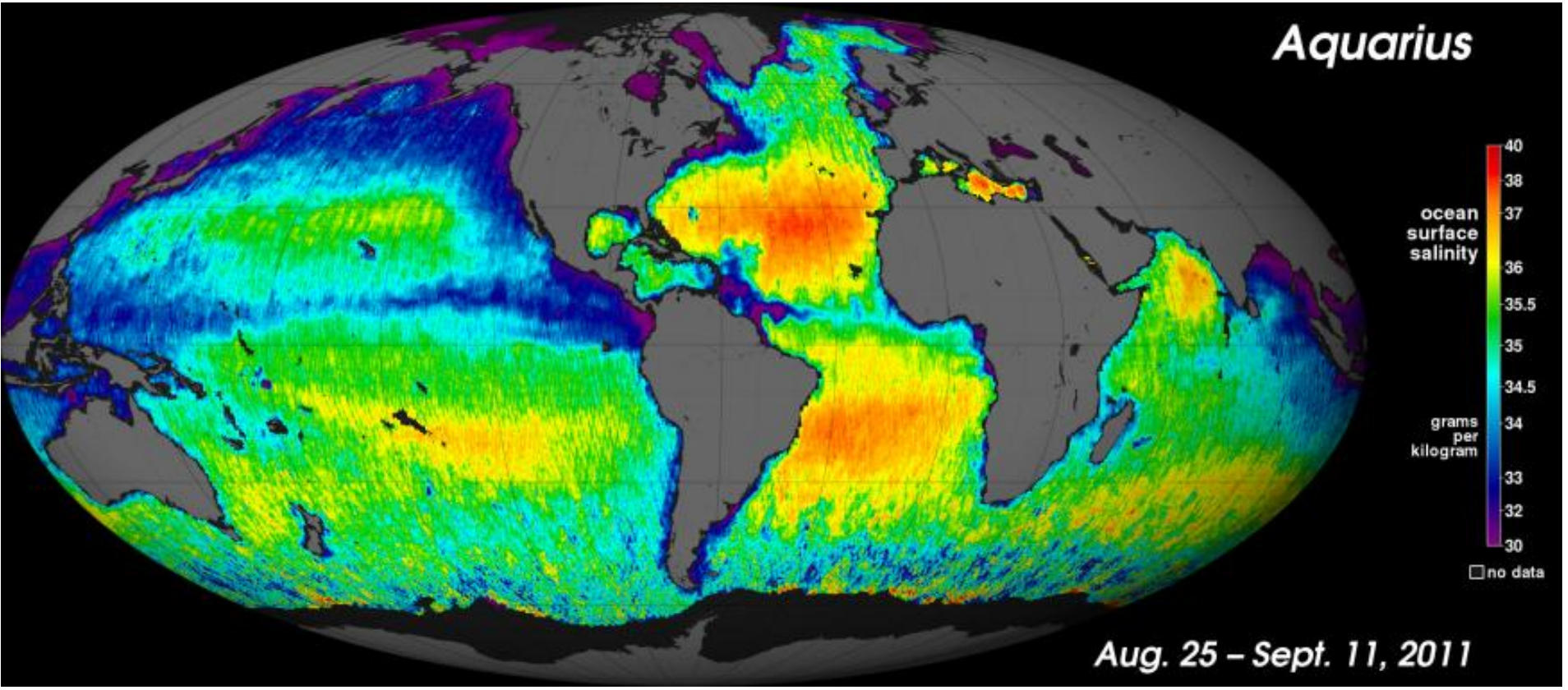

First map of global ocean Sea-surface Salinity from the Aquarius microwave radiometer.

Aquarius Sea-Surface Salinity

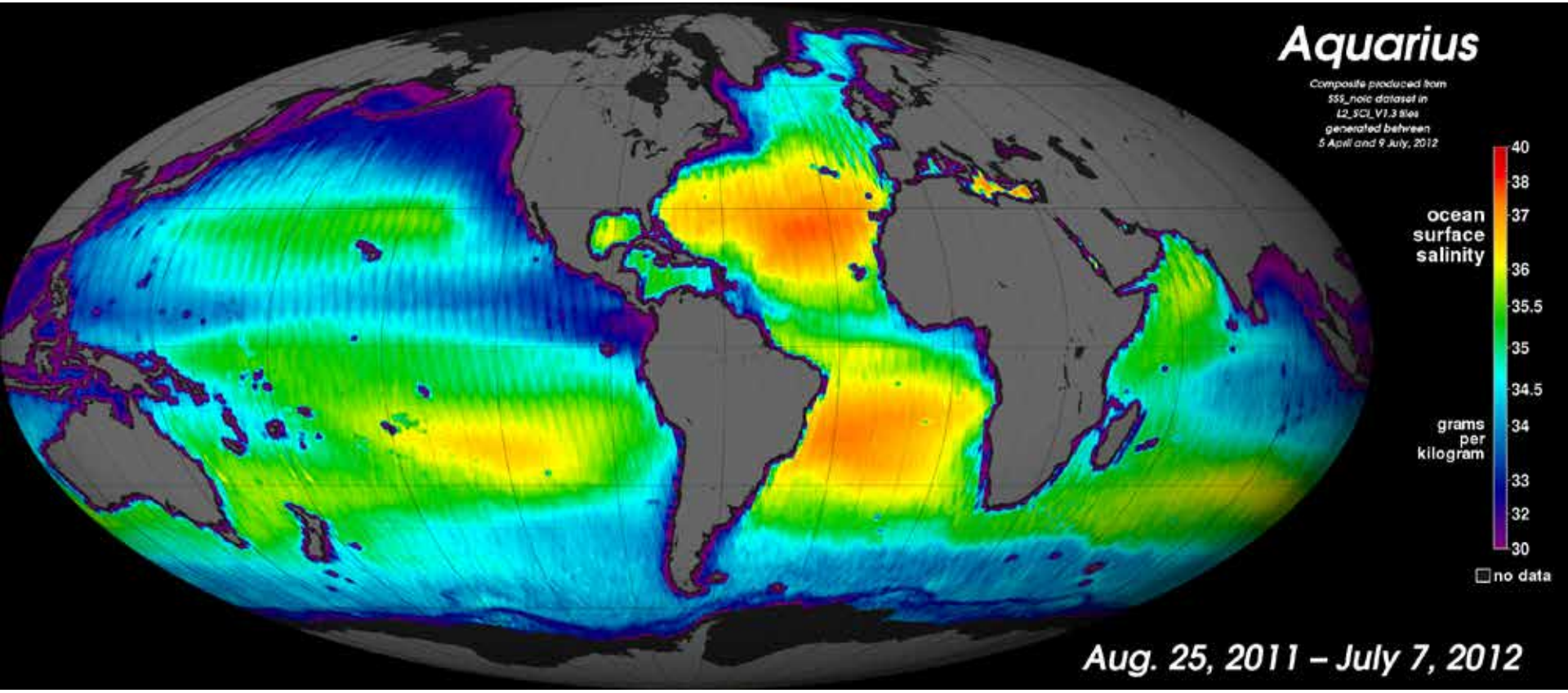

SMOS Sea-Surface Salinity

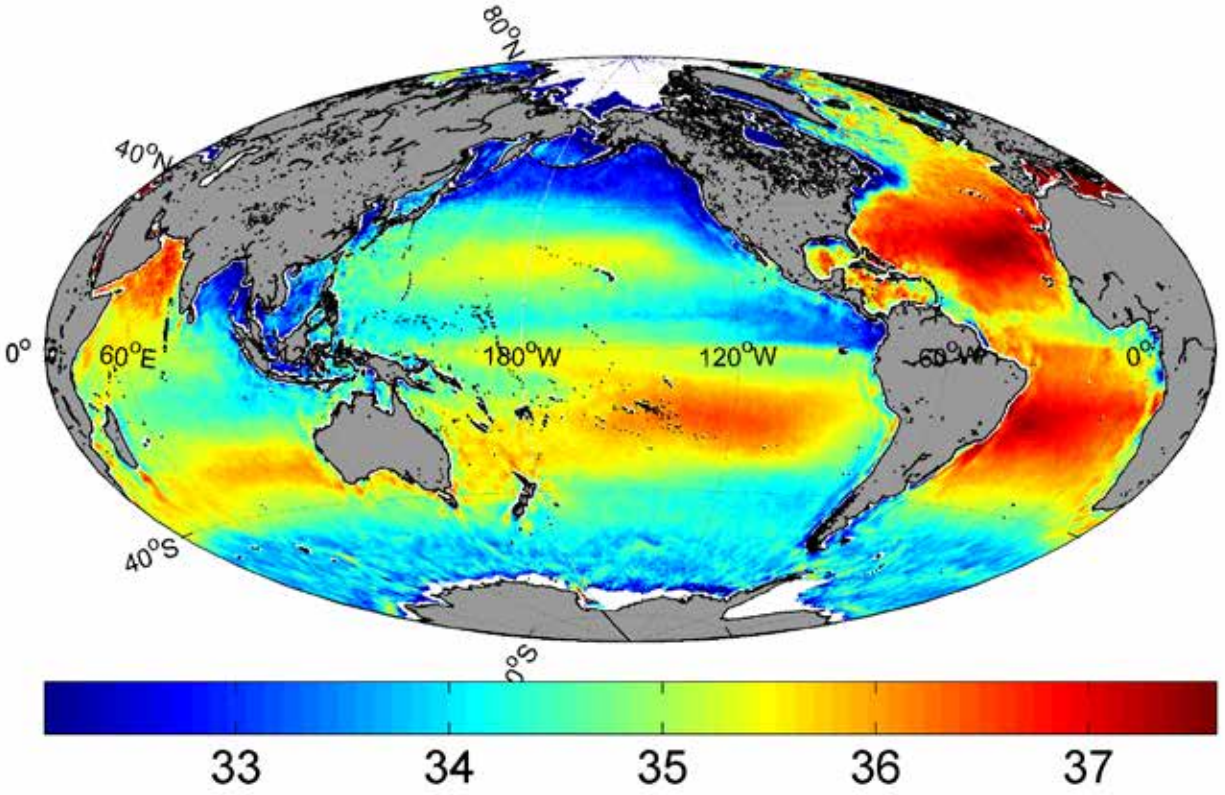

Annual Average Sea Surface Salinity map at 0.25°x0.25° resolution deduced from SMOS satellite data for the year 2010. (http://www.salinityremotesensing.ifremer.fr/)

Useful Texts

GC10.4.R4

Measuring the Oceans from Space: The principles and methods of satellite oceanography Ian Robinson, 2004

An Introduction to Ocean Remote Sensing, Seelye Martin, 2004

Microwave Remote Sensing: Active and Passive (3 vols), Ulaby, F. T., R. K. Moore, and A.K. Fung, 1981-1986

Satellite meteorology: an introduction, Kidder, Stanley Q and Thomas H. Vonder Haar, 1995

Methods of satellite oceanography, Stewart, Robert H. 1985

Introduction to satellite oceanography, Maul, George A, 1985

Oceanographic applications of remote sensing, Ikeda, Motoyoshi and Frederic W. Dobson, 1995

Atlas of satellite observations related to global change, R.J. Gurney, J.L. Foster, C.L. Parkinson (eds), 1993

Our Changing Planet, the View from Space, M. D. King, C. L. Parkinson, K. C. Partington and R. G. Williams (eds), 2007

All for now….

Questions?

Solar contamination

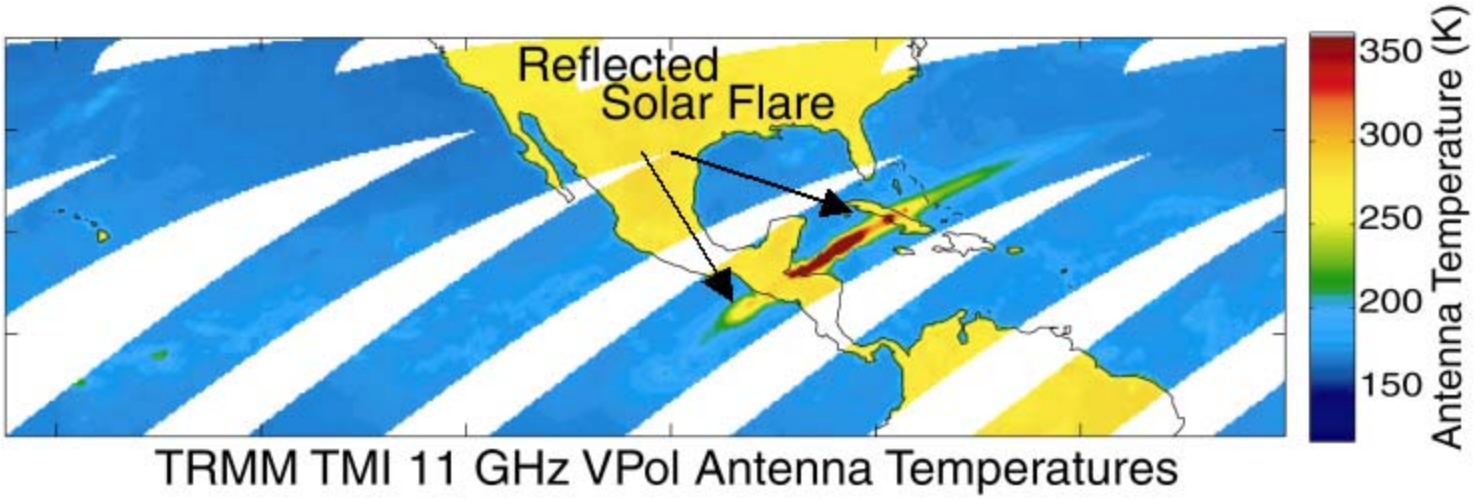

On November 4, 2003, at approximately 19:47 UTC, the largest solar flare event ever recorded erupted. The extremely intense radiation coming from the flare saturated x-ray detectors for 11 minutes. The same hyper-accelerated solar electrons that are responsible for the x-ray burst also emit intense microwave radiation. This burst of solar microwaves, traveling from the sun to the Earth in 8 minutes, reflected off the ocean surface and was seen by the TRMM microwave imager (TMI). The radiation was so intense that it saturated the 11-GHz TMI channels.

Remote Sensing Systems (RSS) detected this event during a routine data quality check that revealed anomalous geophysical retrievals. RSS processes TMI data into a suite of ocean products, including ocean temperature, wind speed, atmospheric water vapor, cloud, and rain rates, for use in weather forecasting, climate modeling, and scientific research. The erroneous ocean retrievals were traced back to exceptionally high microwave radiances coming from the solar flare.

Imagine looking at the ocean on a sunny day. When you look at a certain angle, you see the sun's reflection. This angle is the specular reflection angle. Occasionally the satellite's viewing angle matches the specular reflection angle. Serendipitously, TMI was looking at the specular reflection of the sun at the time of the solar flare event. The 11-GHz solar reflection as seen by TMI increased more than 100-fold during the 11-minute flare.

http://www.remss.com/rss_research/tmi_solar_flare.html

MODIS 4µm SST Composite

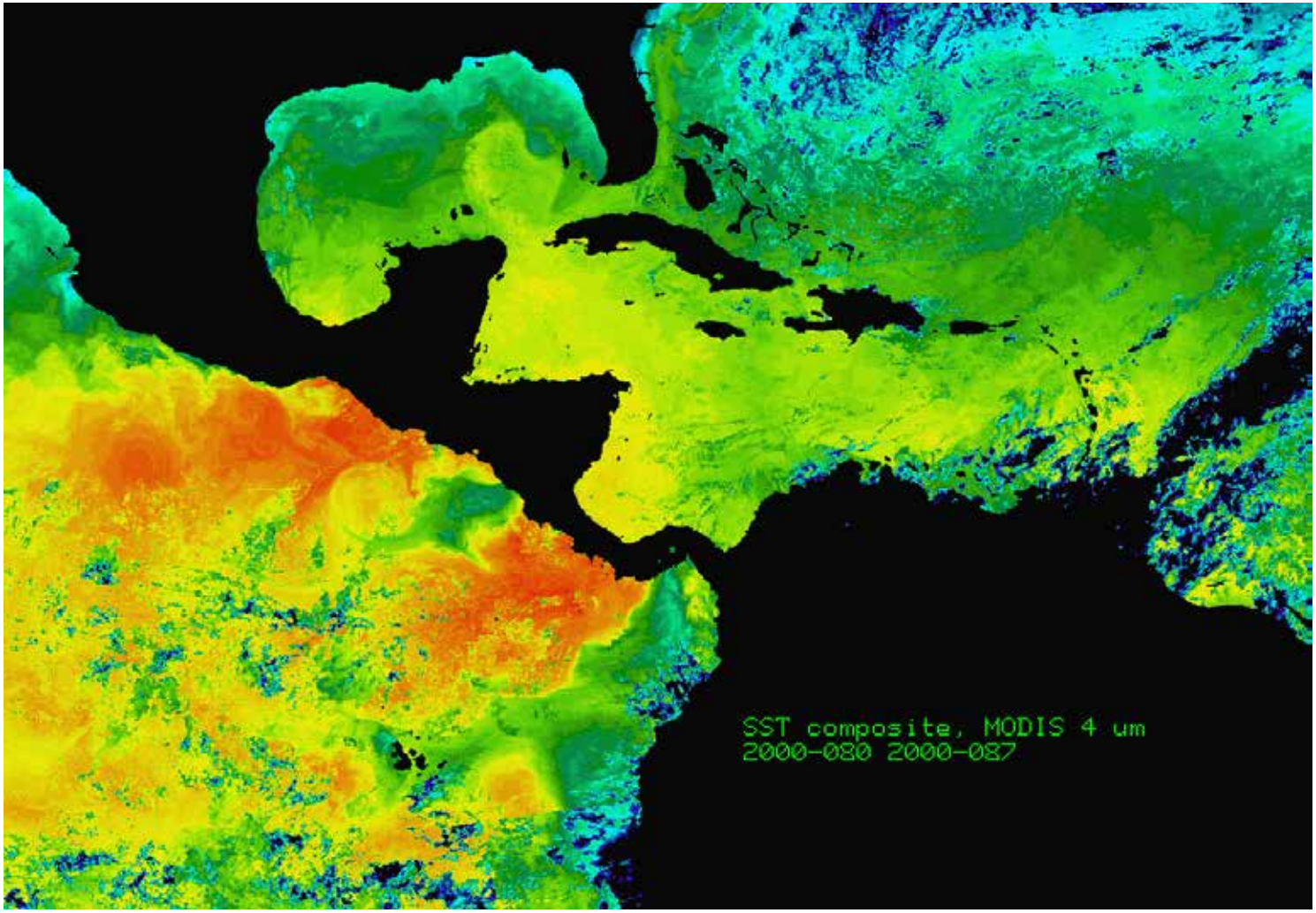

Integrated water vapor

Coefficients in algorithm are derived by comparison with radiosonde measurements.

These are also used to determine the accuracy of the microwave retrievals.

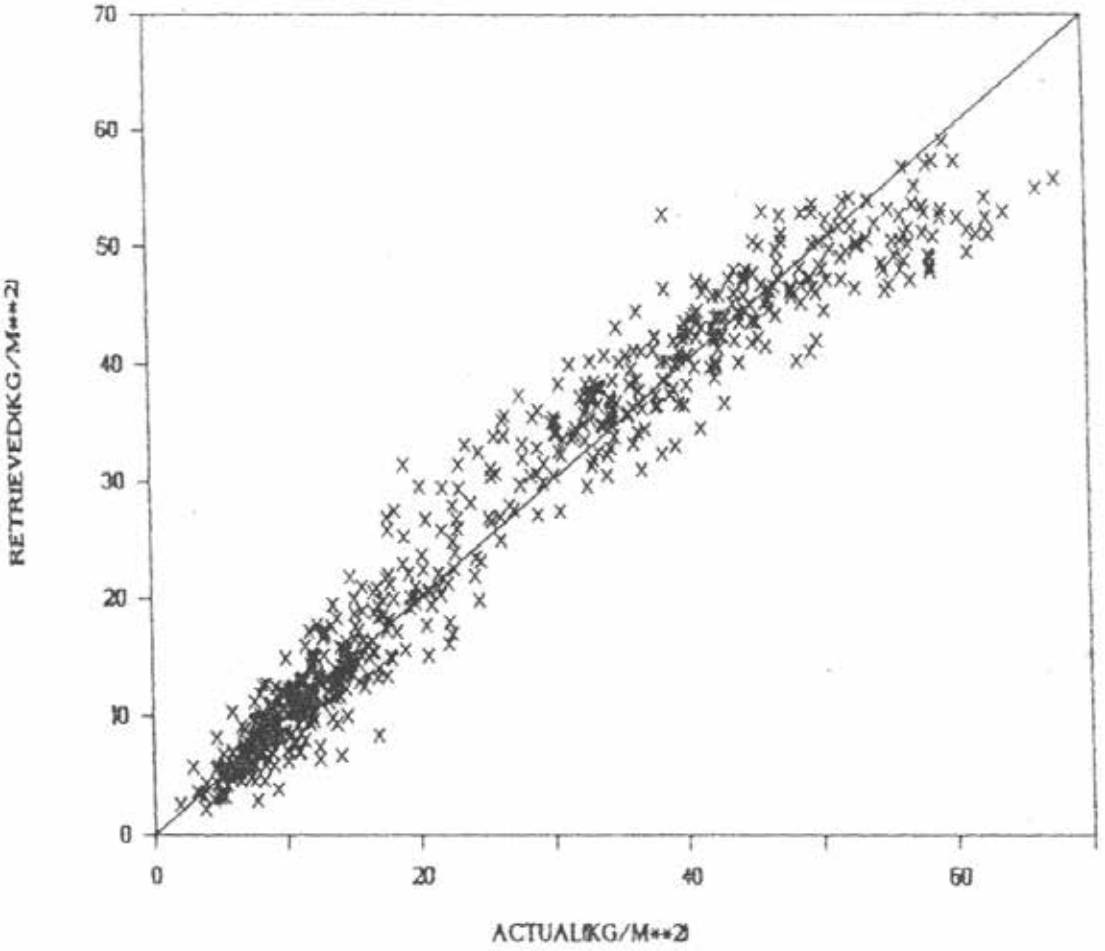

Fig. 5. Retrievals from a linear global algorithm developed at NESDIS versus raobs. Units are in kg/m^2 or precipitable millimeters. The linear algorithm has significant nonlinearities in the retrievals. It shows a tendency to overestimate at medium values and to underestimate at large values.

Planck Function

In searching for a theoretical derivation of blackbody radiation, Planck made the revolutionary assumption that an oscillating atom in the wall of a cavity can exchange energy with the radiation field inside a cavity only in discrete bundles called *quanta* given by $\Delta E = h\nu$, where h is known as *Planck's constant*.

With this assumption, he showed that the radiance being emitted by a blackbody is given by

$$B_\lambda(T) = \frac{2hc^2\lambda^{-5}}{\exp\left(\frac{hc}{\lambda kT}\right) - 1}, \qquad (3.7)$$

where k is Boltzmann's constant, and T is the absolute temperature.

This is the *Planck function*; it earned him the Nobel Prize in 1918. The Planck function is more conveniently written as

$$B_\lambda(T) = \frac{c_1\lambda^{-5}}{\exp\left(\frac{c_2}{\lambda T}\right) - 1}, \qquad (3.8)$$

where c_1 and c_2 are the first and second radiation constants.

Since the radiance from a blackbody is independent of direction, the radiant exitance from a blackbody is simply πB_λ.

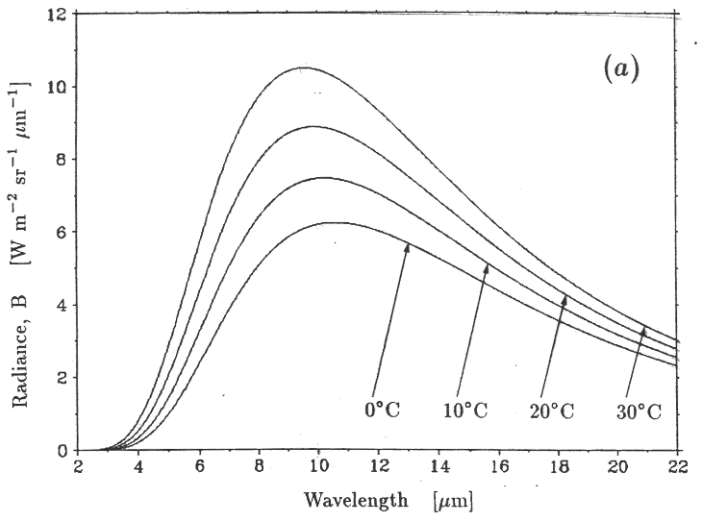

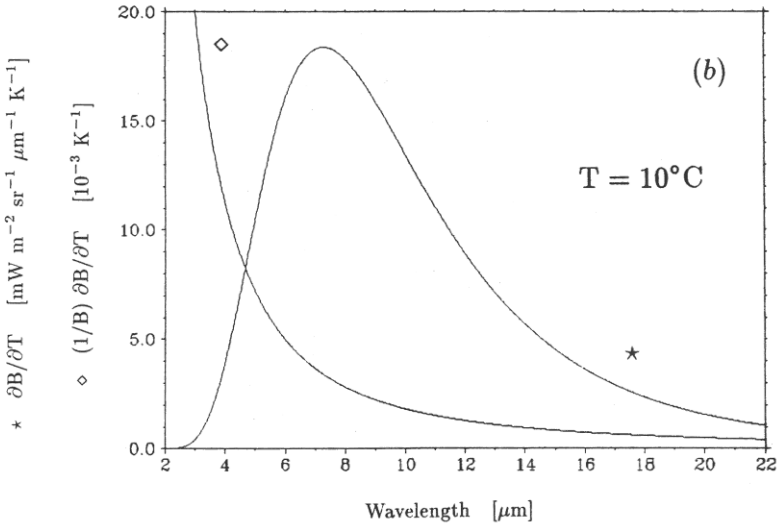

DMSP Sensors

OLS - Operational Linescan System

SSM/I - Special Sensor Microwave Imager (on F-17 this is replaced with SSMIS - Special Sensor Microwave Imager/Sounder)

SSM/T - Special Sensor Microwave Temperature Sounder (not on F17)

SSM/T-2 - Special Sensor Microwave Water Vapor Profiler (not on F17)

SSIES - Special Sensor Ion and Electron Scintillation Monitor

SSJ/4 - Special Sensor Precipitating Electron and Ion Spectrometer

SSB/X-2 - Special Sensor Gamma/X-Ray Detector

SSM - Special Sensor Magnetometer

Defense Meteorological Satellite Program (DMSP)

Satellite F17

DMSP Satellite F17 is in a near circular, sun synchronous, polar orbit.

- temporal coverage: 4 November 2006 to present
- maximum altitude: 855 km
- minimum altitude: 841 km
- inclination: 98.8 deg
- period: 102.0 minutes
- eccentricity: 0.00096
- ascending equator crossing time (local time):
  - at launch: 17:31
- swath width:
  - visible and infrared imagery: 3000 km
  - microwave imagery: 1400 km
  - temperature sounder: 1500 km
  - water vapor profiler: 1500 km
- launch date: 04 November 2006

Time of measurement

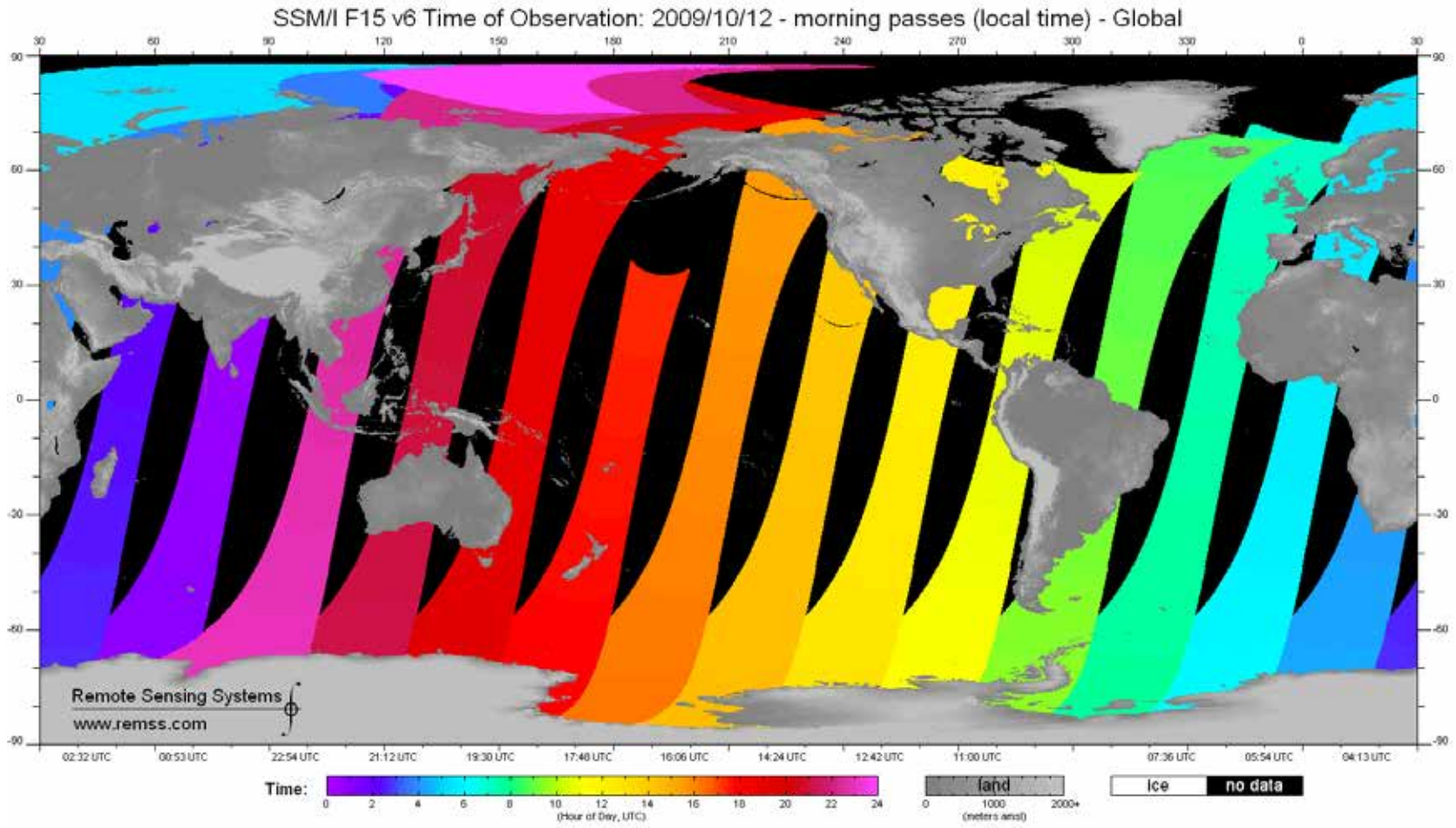

Remote Sensing Systems
www.remss.com

AMSR-E Ocean Products

AMSR-E

Wind Speed

SST

Rain Rate

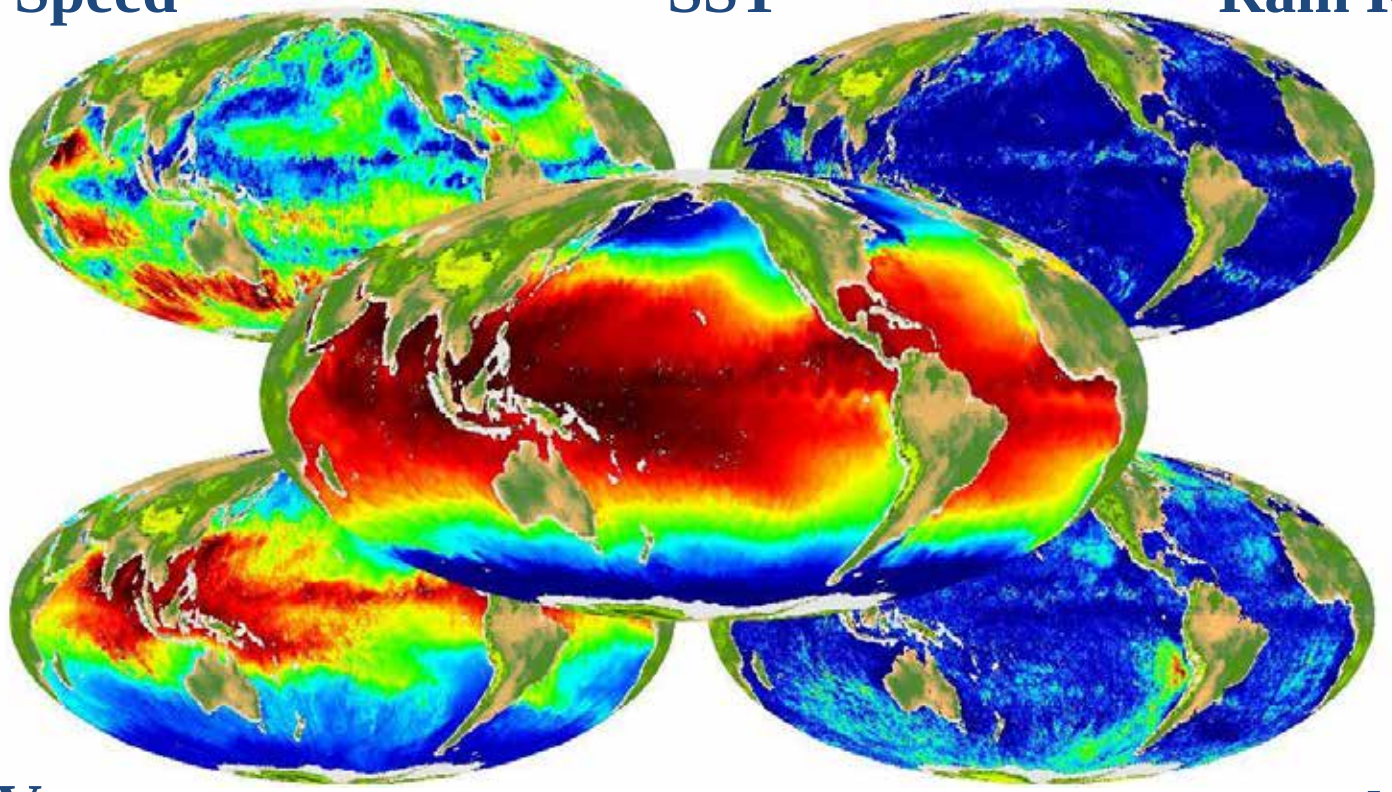

Water Vapor

Cloud